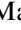








## STABLE ISOTOPIC ANALYSIS AND RADIOCARBON DATING OF *MICROPOGONIAS FURNIERI* OTOLITHS (SCIAENIDAE) FROM SOUTHEASTERN BRAZILIAN COAST: SEASONAL PALAEOENVIRONMENTAL INSIGHT

Mariana Samor Lopes<sup>1\*</sup>  • Elise Dufour<sup>2</sup>  • Elisamara Sabadini-Santos<sup>3</sup>  • Maria Dulce Gaspar<sup>4</sup>  • Kita Macario<sup>5</sup>  • Bruna da Silva Mota Neto<sup>5</sup> • Olivier Tombret<sup>2</sup> • Denis Fiorillo<sup>2</sup> • Michel Lemoine<sup>2</sup> • Leandro Amaro Pessoa<sup>6</sup> • Sandrine Grouard<sup>2</sup>  • Orangel Aguilera<sup>1</sup> 

<sup>1</sup>Departamento de Biologia Marinha, Universidade Federal Fluminense (UFF), Laboratório de Paleocologia e Mudanças Globais (LP&MG). Campus Gragoatá, Bloco M, 24210-201, Niterói, RJ, Brazil

<sup>2</sup>Archéozoologie, Archéobotanique : sociétés, pratiques, environnements (AASPE) UMR 7209 Muséum national d'Histoire naturelle, CNRS, 55 rue Buffon, 75005 Paris cedex 05, France

<sup>3</sup>Departamento de Geoquímica, Universidade Federal Fluminense, Outeiro São João Batista, s/n, Niterói, 24001-970, RJ, Brazil

<sup>4</sup>Programa de Pós-Graduação em Arqueologia do Museu Nacional (PPGARq), Universidade Federal do Rio de Janeiro (UFRJ), Quinta da Boa Vista, s/n, Rio de Janeiro, 20940-40, RJ, Brazil

<sup>5</sup>Laboratório de Radiocarbono, Instituto de Física, Universidade Federal Fluminense, Av. Gal. Milton Tavares de Souza s/n, 24210-346, Niterói, RJ, Brazil

<sup>6</sup>Departamento de pesquisa e engenharia, Instituto Virtual Internacional de Mudanças Globais (IVIG- COPPE / UFRJ), Universidade Federal do Rio de Janeiro (UFRJ), Cidade Universitária, Avenida Pedro Calmon s/n, 21941-596, RJ, Brazil

**ABSTRACT.** Isotopic analysis of *Micropogonias furnieri* otoliths were used to get insight into palaeoceanographic conditions in the Guanabara Bay and Saquarema Lagoon, Rio de Janeiro state (RJ), located on the southeastern coast of Brazil, under upwelling influence of the Cabo Frio system. Archaeological otoliths come from two Holocene shellmounds (or *sambaquis*): Galeão and Beirada. For the first time, radiocarbon analysis using high accuracy techniques were performed at Galeão. Age range was determined to be between 5820 and 4980 cal BP, which extends the chronology of human settlement in the Guanabara Bay. Micro-samples of the otoliths were collected sequentially from the core to the edge, to provide continuous  $\delta^{18}\text{O}$  and  $\delta^{13}\text{C}$  isotopic profiles over the lifetime of the individual fish. Derived- $\delta^{18}\text{O}_{\text{oto}}$  palaeotemperature estimates vary according to seasonality, resulting in a palaeoceanographic variation between 8 to 31°C for Guanabara Bay and 8 and 28°C for the Saquarema Lagoon. Our data indicate that whitemouth croakers were captured during the Middle Holocene from the Guanabara Bay and Saquarema Lagoon and resided in cooler temperatures compared to temperatures of current conditions.

**KEYWORDS:** Atlantic, Holocene water masses, Palaeoceanography, Palaeothermometer, upwelling, whitemouth croaker.

### INTRODUCTION

All regions in the world are affected by global climatic perturbations linked to the interaction between the ocean, the biosphere, and human activities. Climatic and environmental changes have a significant impact on biodiversity and the availability of resources, with their impact on the environment and societies being a major challenge for the coming decades (Barange and Perry 2009; Reid et al. 2009). Since the beginning of the Holocene, archaeological human populations have settled in coastal environments and their zooarchaeological accumulations have recorded the climatic variations of the environment (Grouard 2010).

Atlantic South American coastal ecosystems are diverse, and their environments are changing over time. Their diversity is the consequence of variation in local geomorphology and global climatic changes. Examples from past records show that natural climate changes have affected the oceanic hydro-systems and natural ecosystems, and in particular their biodiversity and their biogeographical distribution (Murawski 1993; Nye et al. 2009). Tracking variations in past

\*Corresponding author. Email: [Lopes\\_mariana@id.uff.br](mailto:Lopes_mariana@id.uff.br)

oceanographic conditions in southeastern Brazil coast is essential to understanding long term environmental and climatic variations in the region, once scarce studies are available. Past changes can be tracked through variations in the biodiversity of zooarchaeological remains and the measurement of their biogeochemical composition such as stable isotopic ratios in carbon and oxygen ( $\delta^{13}\text{C}$  and  $\delta^{18}\text{O}$ ) in an established chronological time frame (Kerr et al. 2007). The coast of the state of Rio de Janeiro contains a large quantity of archaeological shellmounds (called *sambaquis*). These archaeological sites provide evidence of coastal human settlement and activities (Figuti 1993; Gaspar 1999). They are dated approximately between 8000 and 1000 cal BP (Lima 1999–2000; Gaspar et al. 2008; Tenório et al. 2008; Lopes et al. 2016; Carvalho et al. 2018) covering a large portion of the Holocene. The construction of these shell mounds is related to funerary ritual that involved the deposition of a large amount of animal remains (Fish 2000; Gaspar et al. 2013; Klokler 2016). The faunal remains from shellmounds consist of mollusk shells, shark teeth and vertebrae, teleost fish bones and otoliths (“ear stones”), and mammal bones and teeth. Their stable isotope values can be used to get an insight into past oceanographic conditions (Patterson 1998).

Otoliths are metabolically inert structures composed of calcium carbonate ( $\text{CaCO}_3$ ), usually in the aragonite form (Degens et al. 1969; Campana and Neilson 1985). They grow continuously throughout the life of fish and present periodic growth marks (Campana and Neilson 1985). Oxygen isotopes are deposited in equilibrium with ambient water isotope value ( $\delta^{18}\text{O}_w$ ) and temperature (Patterson et al. 1993; Thorrold et al. 1997), while carbon isotopes deposition depends on both fish metabolism and isotopic value of dissolved inorganic carbon (DIC) (Dufour et al. 2007). The  $\delta^{18}\text{O}$  of otolith values ( $\delta^{18}\text{O}_{\text{oto}}$ ) also depend on the isotopic composition of the water mass ( $\delta^{18}\text{O}_w$ ) where the fish resided during their growth. Records of chemical conditions of water masses through  $\delta^{18}\text{O}$  and  $\delta^{13}\text{C}$  values of ancient otoliths can thus be used to reconstruct past freshwater (Patterson 1998; Dufour et al. 2018) and marine environments (Price et al. 2009; Bertucci et al. 2018). Otoliths were previously used to reconstruct variation in mean temperature during the Late Holocene for two locations of the Rio de Janeiro coast: the Cabo Frio oceanographic system and Saquarema Lagoon (Bertucci et al. 2018).

Developments in microscopic sampling techniques associated with mass spectrometry enabled the measurement of intra-otolith isotope variations (Begg and Weidman 2001; Wurster et al. 2005). Applying sequential sampling and isotopic analysis to well-preserved otoliths from southeastern Brazilian shellmounds provides the opportunity to get an insight into past water mass conditions at a seasonal scale.

Despite a strong option for using shell or charcoal samples for radiocarbon dating in archaeology, fish otoliths have been successfully dated in numerous studies (Scartascini and Volpedo 2016; Carvalho et al. 2018). Otoliths have the potential to confirm the absolute age of individual fish, in addition to their potential to serve as proxies for studies of both seasons of site occupation and palaeoclimatic conditions.

In the present study, we analyzed whitemouth croaker (*Micropogonias furnieri*) otoliths recovered from two Holocene shellmounds of southeastern Brazil, Rio de Janeiro state, namely Beirada and Galeão, located near the Saquarema Lagoon and the Guanabara Bay, respectively. Zooarchaeological records associated with the Beirada and Galeão shellmounds (Kneip 2001; Lopes et al. 2016, 2022) indicate that fishing was a common

activity in these sites. Estuarine resources commonly found in these shellmounds include *Archosargus* sp., *Bagre* spp., *Centropomus* spp., *Chaetodipterus faber*, *Cynoscion* spp., *Caranx* spp., *Epinephelus* sp., *Micropogonias furnieri*, *Pogonias courbina*, and several sharks. Although there is no record of the offshore teleost fishery at these sites, this activity around Galeão shellmound has not been ruled out (Lopes et al. 2022). Whitemouth croaker has been the most abundant resource recorded in these two settlements in prehistoric times (5600–900 cal BP; Kneip et al. 2001; Lopes et al. 2016; Gaspar et al. 2018) and are still the most abundant demersal fishing resources in Brazil (Carneiro et al. 2005; Rodrigues et al. 2007). This study has four major goals: (1) to provide for the first time a chronology for the Galeão shellmound through <sup>14</sup>C dating, (2) to check the aragonite preservation of otoliths from the Galeão shellmound by SEM examination of the microstructure in transverse polished sections, (3) to recreate the lifecycle of the fish on the seasonal scale through sequential sampling and isotopic analysis of the otoliths annuli, and (4) to reconstruct Holocene palaeotemperature and characteristics of water masses of the Guanabara Bay and Saquarema Lagoon through intra-otolith profiles of  $\delta^{18}\text{O}$  and  $\delta^{13}\text{C}$  values.

## MATERIAL AND METHODOLOGY

### Study Sites and Archaeological Sites

The Guanabara Bay and the Saquarema Lagoon complex are two coastal shallow water environments in southeastern Brazil (Figure 1).

The oceanographic setting of the coastal shelf of southeastern Brazil is controlled by three main water masses: Subtropical Shelf Water (SSW), which is found on the inner shelf (>20°C; 35–36 salinity and 30 m depth); the warm and saline surface of the Tropical Water (TW) on the outer shelf (24–28°C; 37 salinity and 0–200 m depth) and the Central South Atlantic Water (SACW) in the middle platform (18°C; 35–36.4 salinity and 110 m depth) (Cordeiro et al. 2014). The Guanabara Bay and Saquarema Lagoon are both under the influence of the seasonal upwelling system that develops off the shores of the city of Cabo Frio. This system is associated with the emergent deep and colder SACW, a consequence of NE winds and the coastal geomorphology of the region (Souto et al. 2011; Belem et al. 2013).

The Guanabara Bay is a semi-enclosed coastal ecosystem (Amador 1980) connected to the Atlantic Ocean through a strait channel (Catanzaro et al. 2004). It has a surface area of 328 km<sup>2</sup> (Kjerfvee et al. 1997), which is mostly (84%) characterized by shallow water (ca. 10 m deep) (Figueiredo et al. 2014) (Figure 1). The oceanographic conditions, temperature and salinity vary seasonally, with seasonal variation in air temperature and pluviometry exhibiting large amplitudes (Table 1, Figure 2) (Eichler et al. 2003; Soares-Gomes et al. 2016; Kjerfvee et al. 1997; World Ocean Atlas Dataset 2018; Giovanni: NASA 2019).

The Galeão shellmound was built on the western side of the Guanabara Bay approximately 900 m away from the shoreline on a hill of the coastal massifs (CNSA 2018). Site excavation was conducted by M. Gaspar in 2015, at the Tom Jobim International Airport in Ilha do Governador (22°82'02"S, 43°24'05"W). This site was described by Gaspar (2015) but had not yet been dated.

The Saquarema Lagoon system is complex, composed of four interconnected lagoons (Urussanga; Jardim; Boqueirão and De Fora), with an average depth of 1.30 m and a

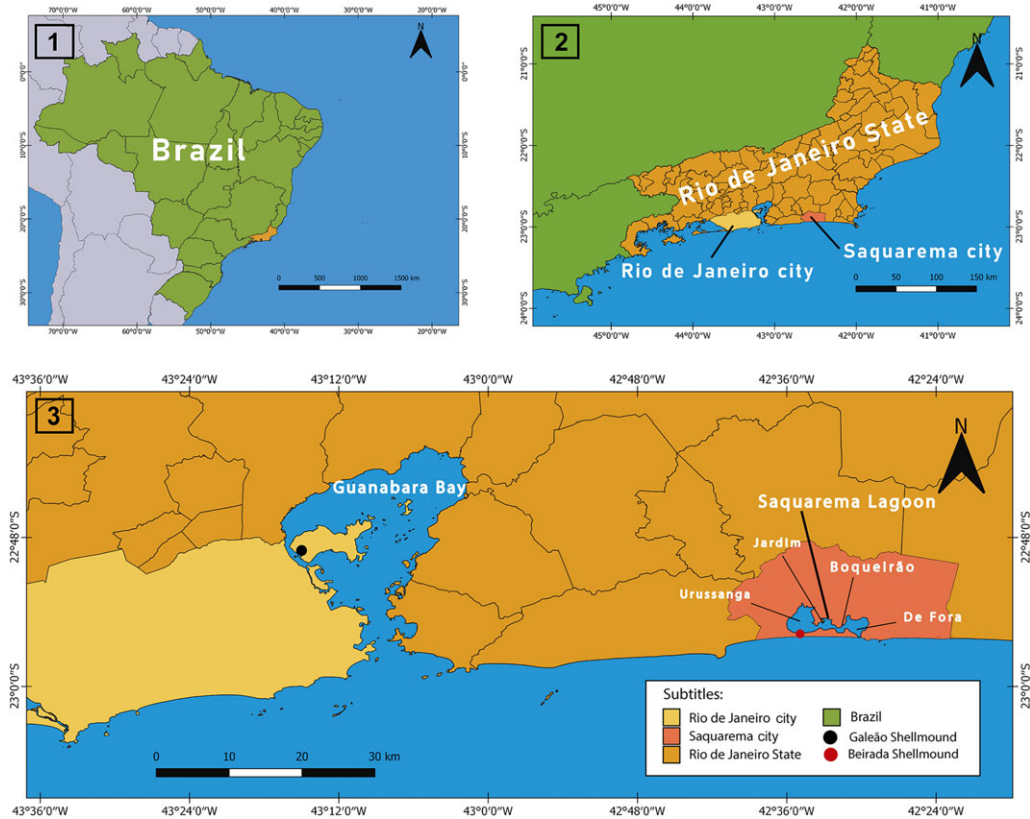


Figure 1 Study area along the southeastern Brazilian coast showing the shellmound locations: (1) Brazil map; (2) Rio de Janeiro State covering Rio de Janeiro city and Saquarema city; (3) Galeão shellmound located at Guanabara Bay and Beirada Shellmound located at Saquarema Lagoon (composed for four connected smaller lagoons).

maximum depth of 2.80 m (Costa-Moreira 1989) (Figure 1). It is located approximately 60 km from the Cabo Frio region. The regional environmental conditions are summarized in Table 1 and Figure 1, following data published by Costa-Moreira (1989), Carmouze et al. (1991), and the World Ocean Atlas Dataset Giovanni database (Giovanni: NASA 2019). There is a wedge of cold water which has developed in Saquarema, under the influence of seasonal upwelling (Carbonel 1998).

The Beirada shellmound (22°92'58"S, 42°54'40"W) was formed over a sandy dune in the coastal plain contiguous to the Saquarema Lagoon (Kneip et al. 1991) (Figure 1). It is located on the sandbank and partially isolated from the coast by an extension of the sandy bar. The width of the sandbank is variable but the shellmound has a total area of 1890 m<sup>2</sup> and its height is 5 m (Kneip et al. 1988).

Unlike the Galeão shellmound, a lot of radiocarbon data are available for the Beirada shellmound. The study of Kneip et al. (1991) indicates an uncalibrated age of 4520 ± 190 BP, and Lopes et al. (2016) support ages varying between 5595–3035 cal BP, close to the data found by Barbosa-Guimarães (2011), which is between 5255 and 3305 BP.

Table 1 Environmental oscillations in salinity; water surface temperature; water surface vertical temperature (0–150 m depth) and annual rainfall of the Guanabara Bay and Saquarema Lagoon surroundings.

Site	Salinity summer (PSU)	Salinity winter (PSU)	WST summer (°C)	WST winter (°C)	WST Guanabara Bay front (°C)	WSVT site front (°C)	Annual rainfall (mm)
Guanabara Bay	13–33	29–34	26–31	22–25	≈22–28	17.31–24.2	1800–2400
Saquarema Lagoon	16–35		≈28–30	≈23–25	≈21–26.5	15.7–24.5	900–1100

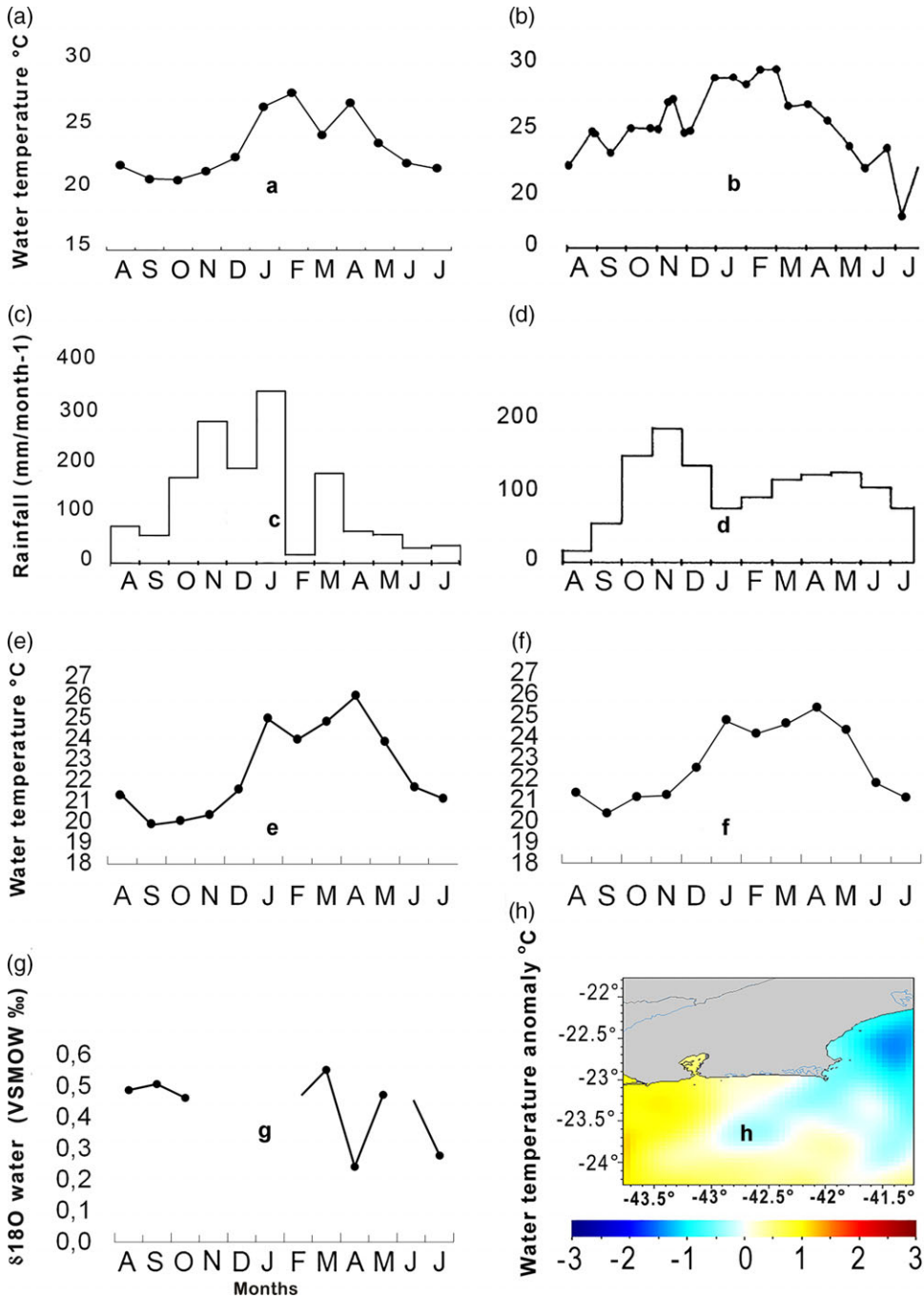


Figure 2 (a) Average annual water surface temperature inside Guanabara Bay; (b) average annual water surface temperature inside Saquarema Lagoon; (c) Average annual rainfall inside Guanabara Bay; (d) average annual rainfall inside Saquarema Lagoon (modified from Carmouze et al. 1991); (e) average annual water temperature on the Guanabara Bay front; (f) average annual water temperature on the Saquarema Lagoon front; (g) available  $\delta^{18}O_w$  data around Saquarema Lagoon front (‰) (data from Venancio et al. 2014); (h) sea surface temperature anomaly – NOAA Global Coral BTeaching Monitoring; 5 km. V.3.1. Monthly. 1995–present; 1999-02-16T00:00:00Z. (Data courtesy of NOAA/NESDIS/STAR Coral Reef Watch program.)

### ***Micropogonias furnieri* Archaeological Otoliths**

The shellmounds are not formed by a continuous horizontal deposition, as this is a dynamic process, in which stratigraphic inversions are common (Fish et al. 2000; Villagran et al. 2010; Gaspar et al. 2013).

A total of eight whitemouth croaker otoliths from the Guanabara Bay were used in this study. The two otoliths that were dated in this article (GS-745 and GS-746), as well as the other otoliths (GS-743, GS-744, GS-1073, GS-1077, GS-762, GS-1151), come from the base of the Galeão shellmound, once the top of this site was destroyed by anthropic changes. As there were not many *Micropogonias furnieri* otoliths due to the high anthropic impact in this site, the sampled otoliths were the largest found in the shell mounds. However, we prioritize the right otoliths (the most numerous). The otoliths selected have different sizes from each other. The GS-743, GS-745, GS-746, GS-762, GS-1073, GS-1077, and GS-1151 otoliths are the right ones, while GS-744 is the left one.

Two otoliths of whitemouth croaker (BS-809 and BS-810) were related to Saquarema Lagoon, from the top of the Beirada shellmound, and both otoliths are the left ones.

### **Whitemouth Croaker Ecology**

Whitemouth croaker otoliths have been previously used as environmental proxies (Volpedo and Cirelli 2006; Aguilera et al. 2016; Bertucci et al. 2018). The biology and ecology of this species is well described in general and specifically for southeastern Brazil (Albuquerque et al. 2012; Franco et al. 2018).

The whitemouth croaker is a long-lived species that can live for over 45 years (Santos et al. 2017) and reach a maximum size of 71 cm (Nakamura et al. 1986; Haimovici and Ignacio 2005). It lives in a maximum water depth of 60 m (Cervigón 1993), preferring temperatures between 16.5 and 28°C (Kaschner et al. 2016) and salinity ranging between 0 and 36 Practical Salinity Unit (PSU) (Franco et al. 2018). Spawning usually occurs on the internal platform and the larvae grow in shallow estuarine environments (Vazzoler 1991; Costa and Araújo 2003; Albuquerque et al. 2012). Three different behaviors are recorded in the coastal areas of Rio de Janeiro as: marine migrant (with a unique movement from the estuarine area towards the adjacent platform in the adult phase); estuarine visitor (with movements from the estuarine area towards the adjacent platform when adult, multiple times throughout their lifespan); and nearshore resident, the most common behavior (with permanence in the adjacent coastal areas influenced by estuarine systems) (Franco et al. 2018).

### **Radiocarbon Dating**

The two otoliths (GS-745 and GS-746) from the base of the Galeão shellmound were first pretreated with HCl and converted to CO<sub>2</sub> by hydrolysis with H<sub>3</sub>PO<sub>4</sub>. The reaction at room temperature overnight, caused the dissolution of CaCO<sub>3</sub> and the release of carbon dioxide (CO<sub>2</sub>). After reaction, CO<sub>2</sub> was purified in a vacuum system and placed in a graphitization tube, where graphite was formed by baking at 550°C for 7 hr (Macario et al. 2016).

Graphite was analysed with a 250 kV SSAMS from the National Electrostatic Corporation, and the isotopic carbon ratios of <sup>12</sup>C, <sup>13</sup>C, and <sup>14</sup>C were determined. Results were normalized using standards taken from the National Bureau of Standards (oxalic acid SRM 4990 c). The radiocarbon age was calibrated using the Oxcal 4.2 software (Bronk Ramsey and Lee

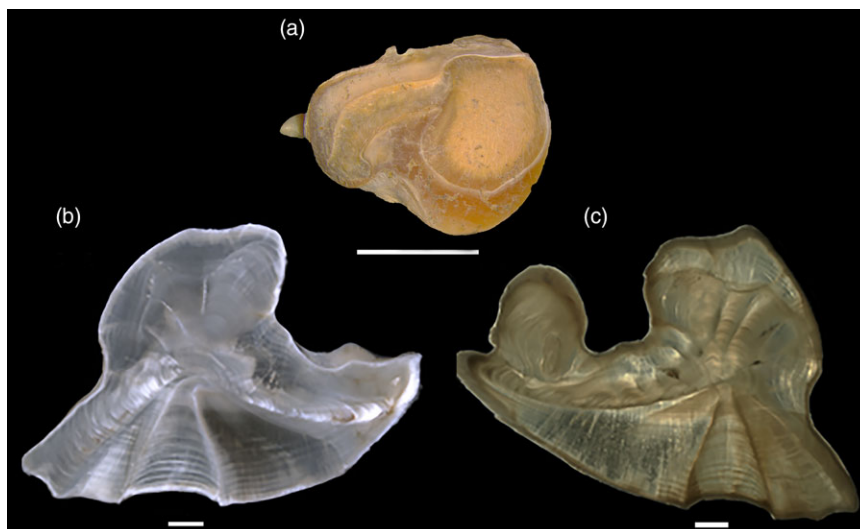


Figure 3 Whole otolith prior to cutting, scale bar 10 mm: (a) image of sample GS-745 in reflected light (b) and transmitted light (c), scale bar of 0.78 mm.

2013), using the Marine20 curve (Heaton et al. 2020) and the reservoir effect correction value  $\Delta R = -270 \pm 130$  calculated for the coast of southeastern Brazil for the period before 4 ka (Macario et al. in prep).

### Annuli Observation

All otoliths—except for the two otoliths from the Galeão shellmound that were used for radiocarbon dating—were cleaned with 70% ethanol and embedded in epoxy resin (Fluka–BioChemica) following the procedure of Secor (1991). Resulting resin blocks were dried at room temperature and cut in cross sections of 0.8-mm thickness, using a low rotation saw (IsoMet). Sections were manually polished using various grit sizes and then were fixed onto glass slides. They were photographed using a stereomicroscope Leica DM RXP in both reflected and transmitted light to observe growth features made of opaque and translucent zones (Figure 3). The opaque zones appear dark in transmitted light and bright in reflected light. The opposite is observed for translucent zones. Opaque and translucent zones are characterized by different relative proportions of calcium carbonate and organic matrix. One opaque and one translucent zone represent one year of growth (Panfili et al. 2002). The formation of translucent zones in whitemouth croaker otolith, when observed in transmitted light, occurs in autumn/winter (May–July) in the Ubatuba Bay, in southeastern Brazil (Santos et al. 2017). In this study, three readers interpreted the annuli reading. Fish size and age estimations methods are available in the Supplemental Material.

### Otolith Preservation

Seven specimens from the Guanabara Bay (GS-743, GS-744, GS-745, GS-746, GS-762, GS-1073, and GS-1151) were examined to evaluate the integrity of the archaeological otolith microstructure. The surface of the sections were etched with acetic acid for 45 seconds in order to reveal growth features (Dufour et al. 2000). For these observations,



Scanning Electron Microscope (SEM) analyses in the secondary electron mode were performed using a MEB–FEG Zeiss Ultra55 equipped with Leica EM SCD500 at the service of MEB of the Institut de Minéralogie, de Physique des Matériaux et de Cosmochimie (IMPMC), MNHN, Paris. Images were taken at 15.00 kV, with a field of view going from 8.46 mm to 500 µm. Otolith microstructure is characterized by bipartite daily increments made of light (L-Zone) and narrow dark (D-zone) zones (Campana 1984; Campana and Neilson 1985) as well as needle-shaped crystals (Cook et al. 2018). Transects crossing the entire otoliths were examined for each specimen but we especially focused on the external border as it is more prone to diagenetic alteration (Cook et al. 2015).

### Stable Isotopic Analysis of Otoliths

The otoliths that had the most visible growth zones when observed in stereomicroscopy were selected for isotopic analysis: four otoliths from the Guanabara Bay (GS-745, GS-762, GS-1073, GS-1151) and two otoliths from the Saquarema Lagoon (BS-809 and BS-810). Sequential micro-sampling was performed from the core to the edge using a Micromill device (New Wave Research) at the Muséum national d'Histoire naturelle (MNHN) in Paris. Between 30 and 60 sub-samples were generated per otolith according to the size of each specimen. The most visible growth zones were digitized to acquire main sampling paths as a series of three-dimensional coordinates that were interpolated (Gerdeaux and Dufour 2012). Intermediate paths were then calculated, spaced at a distance varying between 47 and 254 µm. Each path was drilled at a depth of 50–90 µm and the resulting powder (corresponding to a sub-sample) was collected manually using a scalpel tip.

Isotopic values of all sub-samples of aragonite were measured with a Delta V Advantage mass spectrometer coupled to a Kiel IV device (Thermo®) at the Service de Spectrométrie de Masse Isotopique (SSMIM) of the MNHN. All results were calibrated using NBS-19 international standards and reported as delta, in parts per thousand (‰) following the Vienna Pee Dee Belemnite standards (VPDB). Each run was comprised of the analysis of 38 aragonite sub-samples and eight measurements of the SSMIM internal laboratory standard (Marble LM). The isotopic values of the internal laboratory standard ( $\delta^{13}\text{C} = +2.13\text{‰}$  and  $\delta^{18}\text{O} = -1.83\text{‰}$ ) are corrected to the international standard NBS-19 ( $\delta^{13}\text{C} = +1.95\text{‰}$  and  $\delta^{18}\text{O} = -2.20\text{‰}$ ). Repeated measurement was used to correct those of sub-samples and to determine the precision of the mass spectrometer that was  $\pm 0.02\text{‰}$  for  $\delta^{13}\text{C}$  and  $\delta^{18}\text{O}$  during measurement of the Guanabara Bay samples, and  $0.05\text{‰}$  and  $\pm 0.03\text{‰}$  during measurement of the Saquarema Lagoon samples for  $\delta^{13}\text{C}$  and  $\delta^{18}\text{O}$ , respectively. For the interpretation of intra-otolith isotopic profiles, a cycle and a peak were defined as the variation between two successive lowest  $\delta^{18}\text{O}_{\text{oto}}$  values observed within each profile, with a larger amplitude characterizing a peak.

### Palaeotemperature Estimation

Relating  $\delta^{18}\text{O}_{\text{oto}}$  values to the succession of growth marks allows us to reconstruct seasonal variations in temperature from intra-otolith isotopic profiles (Høie and Folkvord 2006). However, reconstructing palaeotemperatures from  $\delta^{18}\text{O}_{\text{oto}}$  values is not straightforward since  $\delta^{18}\text{O}_{\text{oto}}$  values also depend on the isotopic composition of the water mass ( $\delta^{18}\text{O}_{\text{w}}$ ) where the fish resided while growing. Whitemouth croakers have three different types of behavior: marine migrant, estuarine visitor, and nearshore resident (Franco et al. 2018). There are variations in  $\delta^{18}\text{O}_{\text{w}}$  values among these habitats. Therefore, it is necessary to

Table 2 Thermohaline coefficients and isotopic end-members for water masses types (Taken and modified from Venancio et al. 2014).

Water mass	Termohaline coefficients		<sup>18</sup> O observed (SD)	VSMOW <sup>18</sup> O	VPDB <sup>18</sup> O
	Temperature (°C)	Salinity		end-member adopted	
SSW	24 <sup>a</sup> /25 <sup>b</sup>	34.2 <sup>a</sup> /34.4 <sup>b</sup>	0.22 (0.06)	0	-0.27
TW	25.75 <sup>a</sup> /27 <sup>b</sup>	37.5 <sup>a</sup> /37.6 <sup>b</sup>	0.88 (0.11)	+1.35	+1.08
SACW	9.65 <sup>a</sup> /10.9 <sup>b</sup>	34.97 <sup>a</sup> /35.1 <sup>b</sup>	0.46 (0.10)	+0.4	+0.13

<sup>a</sup>Values for winter condition (May–October)

<sup>b</sup>values for summer condition (November–April).

determine which habitats the fish frequented over their lifetime before estimating palaeotemperature through  $\delta^{18}\text{O}_{\text{oto}}$  values.

Nevertheless, due to the demersal behavior of this species linked to the strong vertical thermohaline stratification in the bay and the Saquarema Lagoon (Costa-Moreira and Carmouze 1991; Cotovicz et al. 2015), it is possible to establish meaningful derived palaeotemperature estimations using an equation specifically for the mixed water of this region.

In order to estimate temperature based on otolith samples, we used a palaeothermometry equation built for a marine Sciaenidae, the Atlantic croaker (*Micropogonias undulatus*) (Thorrold et al. 1997), that was adapted for wild withemouth croaker (Bertucci et al. 2018):

$$\delta^{18}\text{O}_{\text{oto}} - \delta^{18}\text{O}_{\text{w}} = 3.32 - 0.21*(T^{\circ}\text{C})$$

$\delta^{18}\text{O}_{\text{w}}$  is the  $\delta^{18}\text{O}$  value of ambient water in VPDB scale. Water values measured in isotopic standard for water “Vienna Standard Mean Ocean Water” (VSMOW) thus need to be corrected by subtracting 0.27‰ (Hut 1987) before being used in the equation.

The isotopic composition of the main water masses along the Rio de Janeiro continental shelf has been characterized along Cabo Frio and the Guanabara Bay front by Venancio et al. (2014). Consistent differences in  $\delta^{18}\text{O}$  among water masses enable them to be distinguished. Considering there is no isotopic characterization of  $\delta^{18}\text{O}_{\text{w}}$  for the specific regions, we used  $\delta^{18}\text{O}_{\text{w}}$  data measured on the southeastern Brazilian shelf region and adopted for each water mass in VPDB (Table 2).

After calculating water temperature based on Thorrold et al. (1997) using  $\delta^{18}\text{O}_{\text{w}}$  values for three distinct water masses, the relative temperature could be calculated from the percentages quoted for each predominant water mass in this region through the oceanographic mixing model for this upwelling zone (Venancio et al. 2014).

Only oceanographic data collected in up to 60 m depths were considered, since this represents the maximum depth reached by whitemouth croakers (Cervigón 1993). All derived  $\delta^{18}\text{O}_{\text{oto}}$ -palaeotemperature values obtained from the otolith core region were excluded since this could be a result of oscillations modelled by ontogeny in fish (Sadovy and Severin 1994).

Table 3 Conventional radiocarbon ages (BP years) (Stuiver and Polach 1977) and calibrated ages (BP) based on Holocene otoliths of *Micropogonias furnieri* recovered from Galeão shellmound.

Sample ID	Registry name	Radiocarbon age (yr BP)	pMC	Calibrated age (cal BP)
LAC-UFF 190529	GS-745	4949 ± 50	54009 ± 0,333	5720–4980
LAC-UFF 190159	GS-746	5025 ± 43	53498 ± 0,282	5820–4980

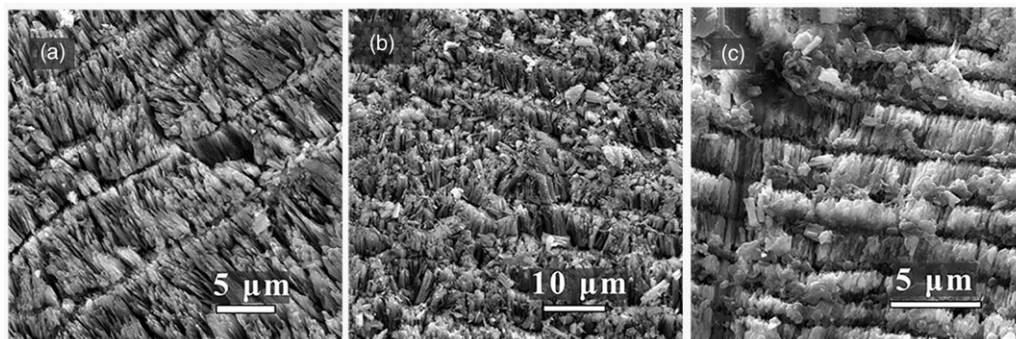


Figure 4 Whitemouth croaker otoliths from the Guanabara Bay; transverse sections: (a) image at the core of specimen GS-743 showing daily increments composed of incremental and discontinuity zones and needle-shaped crystals radially oriented; crystals are interrupting through the discontinuous zone. (b) image of the central zone of sample GS-1073, showing needle-shaped crystals radially arranged. (c) zoomed in image of the edge of sample GS-1151, showing needle-shaped crystals and daily increments.

### Data Treatment

The analyses were performed using the statistical tool R (R Development Core Team 2008). Here we follow criteria using a normality test, a one-way ANOVA and a Tukey post-hoc test to perform a series of comparative analyses: (1) pooled  $\delta^{18}\text{O}$  data (total isotopic values) from Guanabara Bay against  $\delta^{18}\text{O}$  pooled data from Saquarema Lagoon; (2) data of  $\delta^{13}\text{C}$  samples from Guanabara Bay against the of  $\delta^{13}\text{C}$  from Saquarema Lagoon; and (3) the data values of  $\delta^{18}\text{O}$  and  $\delta^{13}\text{C}$  of each sample individually in both locations.

## RESULTS

### Otolith Preservation

None of the analysed otolith sub-samples presented diagenetic alteration by SEM and no evidence of recrystallization was detected. Clear bipartite features representing daily increments perpendicular to the direction of the otolith growth axis are observed, as well as characteristic needle-shaped fibres of aragonite radially oriented are observed at the center, central and border zones (Figure 4, a, b, c).

### Radiocarbon Dating of the Galeão Shellmound

The results of radiocarbon analysis from otolith samples of the Guanabara Bay are available in Table 3 and Figure 5. A previous review reported 17 radiocarbon determinations on nine shell mounds from the region and showed that the occupation of the northeast of the bay occurred

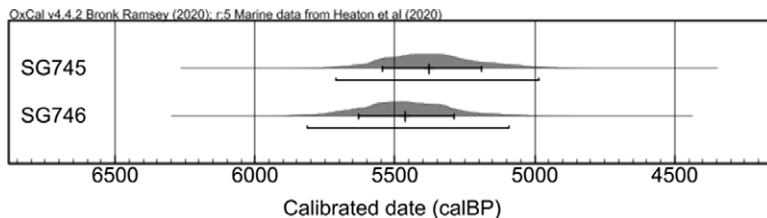


Figure 5 Calibrated ages based on whitemouth croaker otolith samples from top of the Galeão shellmound, using OxCal v 4.2.3 (Bronk Ramsey and Lee 2013). Samples GS-745 (base portion: 60 cm); GS-746 (base portion: 20–50 cm). This figure shows ages obtained by radiochronology (vertical lines). The error bar is represented by horizontal lines.

around 5604–5335 years cal BP (Gaspar et al. 2019). Our results contribute to the chronology of the Guanabara bay shell mounds complex, once it represents an older occupation than report until this time indicating a maximum range varying between 5820–4980 cal BP, with respect to the residual base portion of the shellmound.

### Stable Isotopic Results

Pooled isotopic data of analysed otoliths showed a large range of variation in the  $\delta^{18}\text{O}_{\text{oto}}$  from Guanabara Bay and for  $\delta^{13}\text{C}_{\text{oto}}$  from Saquarema Lagoon specimens (Table 4).

The isotopic data from the Guanabara Bay ranged from  $-4.03$  to  $+3.13$  ‰ and from  $-4.18$  to  $+2.42$  ‰ for  $\delta^{18}\text{O}_{\text{oto}}$  and  $\delta^{13}\text{C}_{\text{oto}}$ , respectively (Figure 6; Appendix I). Analysis reveals no statistical differences in  $\delta^{18}\text{O}_{\text{oto}}$  among samples from four Guanabara Bay specimens ( $F = 1.4463$ ;  $df = 3$ ;  $P = 0.2$ ), and significant differences between  $\delta^{13}\text{C}_{\text{oto}}$  values from these four specimens ( $F = 7.8337$ ;  $df = 3$ ;  $P < 0.01$ ). Tukey post-hoc tests between  $\delta^{13}\text{C}_{\text{oto}}$  showed that the specimen GS-762 differs from the others: GS-762 vs. GS-1073 ( $P < 0.05$ ), GS-762 vs. GS-1151 ( $P < 0.01$ ), and GS-762 vs. GS-745 ( $P < 0.01$ ). Variability in  $\delta^{18}\text{O}_{\text{oto}}$  for the Guanabara Bay specimens suggests that all fish inhabited the same environment, which means that they possibly remained at the Guanabara Bay surroundings, probably mostly inside of the Guanabara Bay. The analysis of fish size, age estimation, and fish movements throughout their life cycle are available in the Supplemental Material.

The isotopic data for the Saquarema Lagoon specimens ( $n = 2$ ) ranged from  $-2.3$  to  $+1.9$  ‰ for  $\delta^{18}\text{O}_{\text{oto}}$  and from  $-7.9$  to  $-1.3$  ‰ for  $\delta^{13}\text{C}_{\text{oto}}$  (Figure 6; Appendix I). Analysis of  $\delta^{18}\text{O}_{\text{oto}}$  between Saquarema Lagoon specimens reveals statistical differences ( $F = 3.8597$ ;  $df = 1$ ;  $P = 0.05$ ), and also shows no correlation between  $\delta^{13}\text{C}_{\text{oto}}$  values of the specimens ( $F = 75.466$ ;  $df = 1$ ;  $P < 0.01$ ). The average amplitudes of  $\delta^{18}\text{O}_{\text{oto}}$  observed is 2.14 (SD = 0.76), higher than in the Guanabara Bay samples (Table 4). However, the range between samples in this site is smaller when compared to the Guanabara Bay specimens  $+4.0$  to  $+3.50$  ‰ and  $+4.60$  to  $+4.80$  ‰ for  $\delta^{18}\text{O}_{\text{oto}}$  and  $\delta^{13}\text{C}_{\text{oto}}$ , respectively (Table 4). The absence of large ontogenetic variation for BS-809 and BS-810 (Figure 7) also suggests that the fish occupied the lagoon region throughout their entire lives.

Analysis of *pooled*  $\delta^{18}\text{O}$  data from the Beirada as compared to the Guanabara Bay specimens reveals significant differences in palaeoceanographic condition signals ( $F = 844$ ;  $df = 1$ ;  $P < 0.01$ ) between these environments, while analysis of pooled  $\delta^{13}\text{C}_{\text{oto}}$  data shows

Table 4 Oxygen isotopes data ( $\delta^{18}\text{O}$  and  $\delta^{13}\text{C}$ ) obtained from growth zones of whitemouth croaker otoliths. The cyclic amplitude in  $\delta^{18}\text{O}$  is expressed as the mean (SD) of the range between the highest (Max) and the lowest (Min) values of each  $\delta^{18}\text{O}$  cycle. SD: standard deviation. Min: Minimum values observed; Max: maximum values observed.

$\delta^{18}\text{O}$ (‰ VPDB)					Mean $\delta^{18}\text{O}$ cyclic variability (‰ VPDB)		
Samples	Mean (SD)	Min	Max	$\delta^{18}\text{O}$ range	Min (SD)	+Max (SD)	Amplitude (SD)
GS-745	-0.65 (0.55)	-3.00	+1.59	4.59	-1.07 (0.68)	-0.09 (0.61)	1.27 (0.27)
GS-762	-0.43 (0.72)	-2.71	+1.87	4.57	-0.30 (0.23)	+0.82 (1.08)	
GS-1073	-0.50 (0.99)	-4.03	+3.13	7.15	-1.18 (0.15)	+0.26 (1.10)	
GS-1151	-0.48 (0.82)	-1.38	+1.37	2.75	-0.70 (0.59)	+0.84 (0.48)	
BS-809	-0.55 (0.73)	-2.30	+1.70	4.00	-1.17 (1.10)	+0.43 (1.12)	2.14 (0.76)
BS-810	-0.05 (1.06)	-2.20	+1.30	3.50	-0.78 (1.25)	+1.90 (1.02)	
$\delta^{13}\text{C}$ (‰ VPDB)					Mean $\delta^{13}\text{C}$ cyclic variability (‰ VPDB)		
Samples	Mean	Min	Max	$\delta^{13}\text{C}$ range	Min (SD)	Max (SD)	Amplitude (SD)
GS-745	0.13 (1.30)	-4.18	+1.74	5.92	-0.19 (1.85)	+0.81 (1.06)	1.82 (1.30)
GS-762	-1.12 (1.16)	-3.46	+1.60	5.06	-1.46 (0.84)	-0.46 (1.33)	
GS-1073	-0.30 (1.06)	-3.68	+2.42	6.09	-1.18 (0.94)	+0.39 (1.14)	
GS-1151	-0.06 (1.15)	-3.55	+1.48	5.02	-2.46 (1.53)	+1.27 (0.30)	
BS-809	-6.05 (1.45)	-7.90	-3.30	4.60	-7.33 (0.56)	-4.88 (1.09)	2.33 (0.25)
BS-810	-3.46 (1.19)	-5.10	-0.30	4.80	-4.38 (0.99)	-2.23 (1.48)	

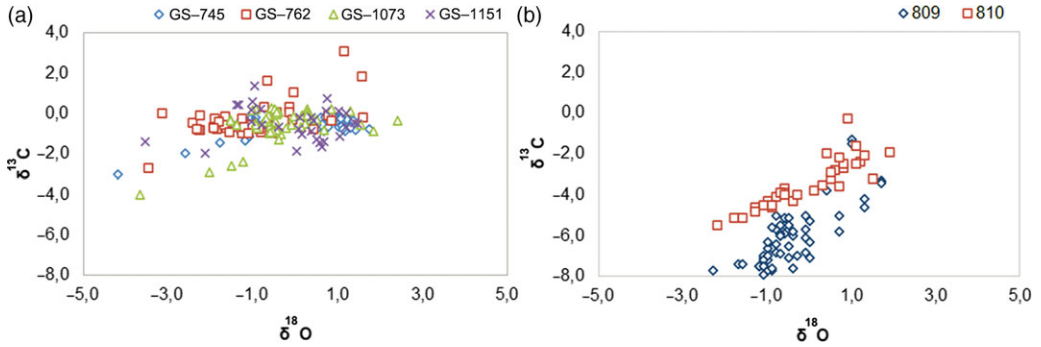


Figure 6 Cross tabulated data of  $\delta^{13}\text{C}$  and  $\delta^{18}\text{O}$  (‰-VPDB): (a) otolith samples from the Guanabara Bay; (b) otolith samples from the Saquarema Lagoon.

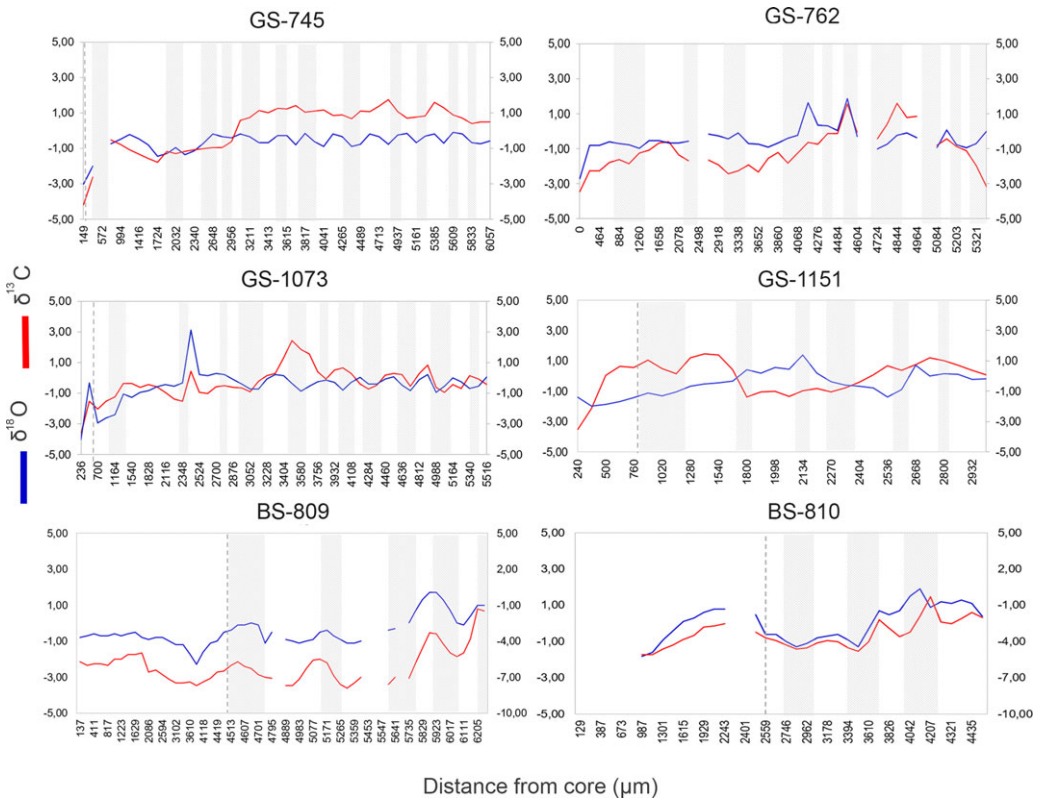


Figure 7 Values of  $\delta^{13}\text{C}$  (‰-VPDB) and  $\delta^{18}\text{O}$  (‰-VPDB) recorded from otoliths of whitemouth croaker of Guanabara Bay (GS) and Saquarema Lagoon (BS).  $\delta^{18}\text{O}$  is shown in blue and  $\delta^{13}\text{C}$  in red. Each graph represents an individual isotopic profile obtained by micro drilling from the core to the edge (left to right) of samples in reflected light. Dark rectangles show samples from autumn/winter (translucent zones). The blank spaces show trends designed for the subsamples that were lost due to insufficient carbonate collected. The dotted lines show the end of the core samples. The sample GS-762 was not sampled in the core once it was difficult the visualization of the growth bands. (Please see online version for color figures.)

similarities ( $F = 3.578$ ;  $df = 1$ ;  $P = 0.06$ ), possibly associated with productivity environments and fish metabolic patterns.

### **Intra-Otolith Isotopic Profiles of the Guanabara Bay**

All individuals from the Guanabara Bay showed similar intra-otolith isotopic profiles over their lives with an ontogenetic change that separates two phases (Figure 7). The first part of the profiles representing the early life phase recorded the lowest  $\delta^{18}\text{O}_{\text{oto}}$  and  $\delta^{13}\text{C}_{\text{oto}}$  values. The second phase was characterized by more or less regular variations made up of cycles and peaks until the death (capture) of the fish. For the specimens studied, the second part of the profiles shows quasi-sinusoidal variations, with 11 complete and one incomplete cycle for GS-745, and nine complete and one incomplete cycle for GS-1073. In addition, GS-1073 presents one large (high) peak in  $\delta^{18}\text{O}_{\text{oto}}$  (Figure 7). The  $\delta^{13}\text{C}_{\text{oto}}$  values also varied but with less regularity for both specimens (Figure 7). The  $\delta^{18}\text{O}_{\text{oto}}$  cycles of GS-762 and GS-1151 were irregular:

GS-1151 showed three  $\delta^{18}\text{O}_{\text{oto}}$  small peaks and GS-762 had four irregular peaks. Moreover, variations in  $\delta^{13}\text{C}_{\text{oto}}$  values were irregular and not synchronous to the  $\delta^{18}\text{O}_{\text{oto}}$  values. The highest  $\delta^{18}\text{O}_{\text{oto}}$  peak range was observed in the first (3.71‰) and third cycles (3.46‰) of GS-1073 reflecting core and spring/summer, respectively and also observed in the first cycle of GS-745 (2.78‰) in spring/summer. Additionally, the highest  $\delta^{13}\text{C}_{\text{oto}}$  ranges in peak values were found in the first peak of GS-1151 (4.60‰), reflecting partially in the core and spring/summer and also the first cycle of GS-745, in spring/summer.

The intra-otolith profiles of the Guanabara Bay specimens had minimum values ranging between  $-4.03$  to  $-1.38$ ‰; and maximum values between  $+1.30$  and  $+3.13$ ‰. The mean  $\delta^{18}\text{O}_{\text{oto}}$  amplitude was 1.27 (SD = 0.27) (Table 4), GS-1151, the youngest specimen, showed the biggest  $\delta^{18}\text{O}_{\text{oto}}$  amplitude ( $+1.54$ ).

### **Intra-Otolith Isotopic Profiles of the Saquarema Lagoon**

Statistical variability in  $\delta^{13}\text{C}_{\text{oto}}$  and  $\delta^{18}\text{O}_{\text{oto}}$  suggests that the two fish recovered at the Saquarema Lagoon experienced different isotopic signals along the Saquarema Lagoon. Contrary to the Guanabara Bay otoliths, BS-809 did not exhibit an ontogenetic shift that separated early and later life phases. The presence of a shift cannot be documented for BS-810, for which the isotope values are missing at the core of the otolith. Large but irregular patterns in  $\delta^{18}\text{O}_{\text{oto}}$  variations are observed for both specimens. At least four complete (one portion of the profile presented missing values) and one incomplete cycle were observed for BS-809 while BS-810 presented at least four complete and one incomplete cycle (Table 4). Nine  $\delta^{13}\text{C}_{\text{oto}}$  cycles were observed for BS-809 and six cycles for BS-810 (Figure 7). Ranges in  $\delta^{13}\text{C}_{\text{oto}}$  of  $+2.3$  and  $3.0$ ‰ were observed on the firsts cycle of BS-809 and BS-810, respectively, which coincide with spring/summer.

The biggest  $\delta^{18}\text{O}$  values are found in an opaque zone for BS-809 and in a translucent zone for BS-810. The highest  $\delta^{18}\text{O}_{\text{oto}}$  peak ranges were observed in the first cycles of BS-809 (partially in the core and autumn/winter) and BS-810 (core). The absence of large ontogenetic variations for BS-809 and BS-810 (Figure 7) also suggests that the fish occupied a lagoon region throughout their lives and had never been in a fully marine environment.

The intra-otolith characteristics of the Saquarema Lagoon specimens show cyclical variations in  $\delta^{18}\text{O}_{\text{oto}}$  values with minimum values ranging between  $-2.30$  and  $-2.20$ ‰, and maximum

values ranging between +1.70 and +1.30‰. The mean values correspond to −0.45 and −0.05 for BS-809 and BS-810. (Table 4). Moreover, the intra-individual variation between the Saquarema Lagoon specimens (+4.0 to +4.10‰) and amplitudes observed (+1.60 and 2.68‰) is higher than in the Guanabara Bay specimens (Table 4).

### **Estimation of Seasonal Water Palaeotemperature Based on Fish Otoliths from Guanabara Bay and Saquarema Lagoon**

The study Venancio et al. (2014) derived  $\delta^{18}\text{O}$  palaeotemperature estimations from the three water masses of the Rio de Janeiro coast: Subtropical Shelf Water (SSW) on the inner shelf, Tropical Water (TW) on the outer shelf, and the Central South Atlantic Water (SACW) in the middle platform.

Using these data, 153 palaeotemperatures were calculated from the isotopic values based in the analysed otoliths from Guanabara Bay. Core values were excluded and considering the values for the SACW water mass (VSMOW = 0.40/VPDB = 0.13‰), the values of the temperatures estimated from the archaeological otoliths ranged from 7 to 30°C. Using the SSW (VSMOW = 0.0/VPDB = −0.27), oscillation was between 5 and 28°C, whereas using the TW (VSMOW = 1.35/VPDB = 1.08), temperatures ranged from 12 to 34°C. The relative temperature calculated from the percentage quoted for each water mass ranged from 8 to 31°C (mean = 19.57°C). The  $\delta^{18}\text{O}_{\text{oto}}$  palaeotemperature records show an overlap between samples (Figure 8a).

Data from autumn/winter range between 8 to 28°C and for spring/summer from 15 to 31°C. The difference between the minimum temperatures for each season suggests a visible seasonal pattern of seasonality of 7°C. The estimated temperature for the capture of fish taken from the average of the last two values of the outer surface, show mean water temperatures of 19.13 (SD = 1.51), during both seasons.

A total of 41 derived  $\delta^{18}\text{O}_{\text{oto}}$ -palaeotemperature values were reconstructed from the Saquarema Lagoon otoliths in Saquarema. For SACW water mass the values estimated ranged between 7 and 27°C. For SSW they ranged between 5 and 25°C, whereas for TW the variation was between 11 and 31°C. Relative palaeotemperatures range between 8 and 28°C (mean: 18.78°C) (Figure 8b). These data suggests seasonal changes, with lower isotopic values occurring in warmer waters and higher values in colder waters.

The amplitudes between winter and summer observed in the samples are, in relative terms, the best indications of seasonal correlations between the two profiles (Figure 7). Values in autumn/winter ranged between 8 and 23°C and spring/summer between 9 and 28°C. The difference between each season's maximum temperatures suggests a seasonal pattern of seasonality of 5°C. Temperature estimation for fish catches was 12°C (SD = 0) (in autumn/winter and spring/summer) for BS-809 and 13.84°C (SD = 2.36) (spring/summer) for BS-810.

## **DISCUSSION**

### **Otolith Aragonite Preservation from the Galeão Shellmound**

Our analysis of external and internal morphology of the Guanabara Bay specimens provides no evidence of diagenesis that could have significantly altered the otolith's stable and radiogenic isotope values. Different morphological, mineralogical and chemical criteria can be used to check the integrity of fossil and archaeological otoliths (Dufour et al. 2000; Cook et al. 2015). When applied to Sciaenidae, they show that otoliths from different archaeological



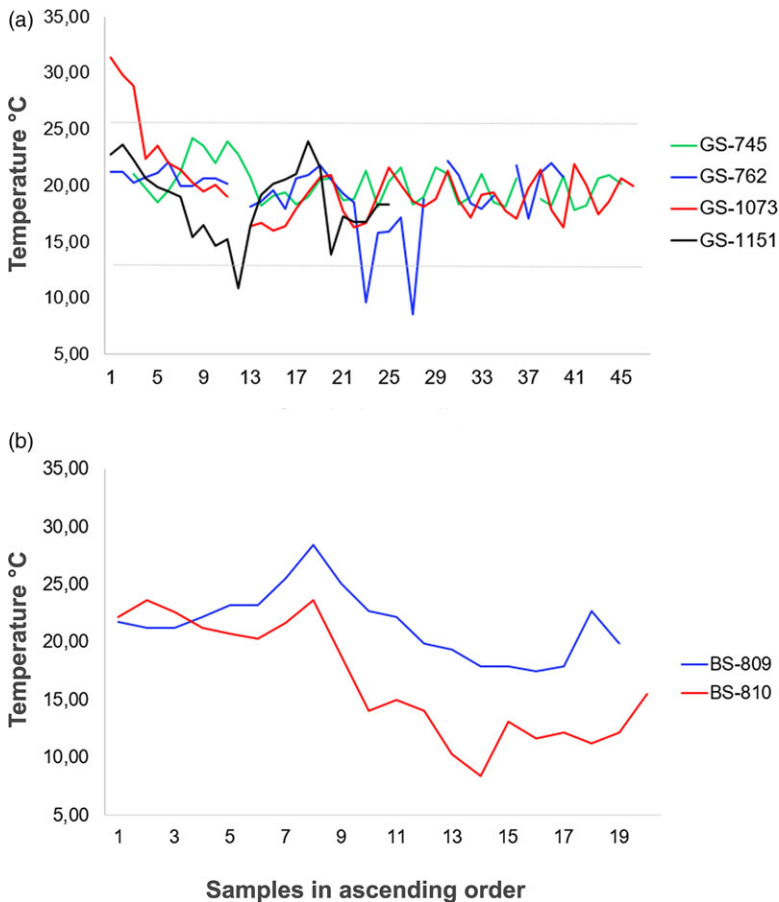


Figure 8 Derived  $\delta^{18}\text{O}$  palaeotemperature: (a) Holocene Guanabara Bay; (b) Holocene Saquarema Lagoon. The  $x$ -axis represents the number of samples in ascending order.

contexts and ages can preserve their integrity (Béarez et al. 2005; Cook et al. 2015, 2016, 2018; Aguilera et al. 2016; Carvalho et al. 2018). Our data further supports the use of Sciaenidae otoliths for accurate dating as well as palaeoenvironmental and palaeoecological reconstructions.

### Shellmound Chronology

Among the 49 shellmounds that have been registered in the Guanabara Bay, so far nine of them have been dated. Data obtained on otoliths from the Galeão shellmound indicated a maximum radiocarbon age range between 5820–4980 cal BP. Previous records obtained from nine studied shellmounds indicated a range between 5584–1620 cal BP (Appendix II; Gaspar et al. 2019). Our new dates partially match the previous records, therefore, our work documents the oldest shellmound settlement of the Guanabara Bay and the oldest phase of occupation of the bay during the Middle Holocene.

The Saquarema region shellmound complex comprises a total of 21 sites, registered at CNSA (2018). Comparison with published data indicates that Beirada shellmound is among the

oldest. Guimarães (2011) published calibrated ages based in many studies and found minimum and maximum data around 4520–1790 BP for sparse sites of the region. A more recent study found otolith data ranging from 4525 to 3640 cal BP, including Manitiba, Saquarema and Ponte do Girau shellmounds and reveal a lower dispersion during the settlement time period in these shellmounds (Carvalho et al. 2018).

The mid-Holocene period is associated with important palaeoceanographic and palaeoclimatic events. There was a higher insolation, correlated with monsoon climates (Pivel et al. 2010). A dryer climate in south eastern Brazil is recorded through change in the sedimentation rate (Figueiredo et al. 2014) and a reduction of gallery forests around 7500–5530 BP (Behling et al. 1995, 2002). The Galeão shellmound is now 5 m above sea level on a rocky island (CNSA 2018). Due to the maximum Holocene transgression (6–5 cal Kbp) the relative sea level was around 3 m above the current one (Amador 1980). The paleobay occupied an area of approximately 800 km<sup>2</sup>, which is twice its current size (Amador 1980). As a consequence, the shellmound was closer to the water line than today but surrounded by shallower water where fishing could have been practiced at a lower energy cost than in the open sea.

On the outskirts of the Beirada shellmound, the maximum sea level variation (+2.5 m) was reached between 4770 and 4490 cal yr BP (Castro et al. 2014), and the external barrier of the Saquarema Lagoon was subject to intense changes (Turcq 1999). The shellmound that is now around 500 m away from the lagoon was located closer to sea in the Holocene period, since it is located in the internal border of the Saquarema Lagoon.

In the Middle Holocene, the configuration of coastal upwelling and SACW middle shelf intrusions in the euphotic zone were already well defined, establishing the modern configuration of the area (Albuquerque et al. 2016). Although Holocene primary productivity has been associated with BC in the mid-shelf portion (Belem et al. 2013; Venancio et al. 2014; Albuquerque et al. 2016), our data support slightly stronger influence of SACW in coastal zones in both seasons, pointing to a cooler and productive waters, which could have favoured fishing, the maintenance of numerous shellmounds in these environments and its builders.

### **Holocene Water Masses of the Guanabara Bay and Saquarema Lagoon**

Despite its relationship to the metabolism of the fish,  $\delta^{13}\text{C}_{\text{oto}}$  values of food are ultimately a function of values of  $\text{DIC}_{\text{water}}$ , and therefore general trends and values can be defined as a characteristic of distinct environments (Patterson 1998). The salinity gradient of riverine and marine waters can be responsible for the overall distributions of  $\delta^{13}\text{C}_{\text{water}}$  isotopic composition of  $\text{DIC}_{\text{water}}$  and can affect the  $\delta^{13}\text{C}$  of the plankton in the estuary (Chanton and Lewis 1999; Druffel et al. 2005). However, the  $\delta^{13}\text{C}$ -DIC signatures in Guanabara Bay did not show conservative distributions with the salinity gradient in the modern bay (Cotovicz et al. 2019). This environment presents a wide range of  $\delta^{13}\text{C}_{\text{w}}$  (–12.2‰ to 4.6‰), lower values are found only around urban outlets or rivers and higher values are found in most parts of the bay (Cotovicz et al. 2019). Kalas et al. (2009) suggests enhanced phytoplankton activity and thus incorporation of  $\delta^{13}\text{C}_{\text{w}}$  with the elevation of  $\text{HCO}_3$  in this bay during winter, while the depleted carbon signature observed in summer could be derived from larger terrestrial inputs.

DIC patterns in the Guanabara Bay's water vary spatially between winter and summer (Cotovicz et al. 2019), this behavior can also mask the clear seasonal changes registered

during fish movements under wide environmental variation. Moreover, the high productivity in Guanabara Bay and Saquarema Lagoon systems are supported by intensive sunlight and elevated temperatures throughout the year. Both belong to the same coastal sector and their respective hydrographic basins are partially linked. In addition, the dependent estuarine behavior of the whitemouth croaker appears to have maintained a close pattern of movement in the past in southeastern Brazilian coast. In conclusion, we can propose the hypothesis that the majority of the archaeological whitemouth croakers of this study were nearshore residents.

Most of the values of  $\delta^{18}\text{O}_{\text{oto}}$  specimens are represented the closest by the characteristics of the SACW, TW, and SSW. However, low isotope values observed can not be characterized in any of the water masses described by Venancio et al. (2014) around the Cabo Frio system. As a result, the range of variation of the isotopes defined for the water masses of the region does not fully explain the low values obtained here. Data provided by Venancio et al. (2014) does not present negative values for  $\delta^{18}\text{O}_{\text{w}}$  and  $\delta^{13}\text{C}_{\text{w}}$  in marine waters in the continental platform between Cabo Frio and the Guanabara Bay front, which reinforces the persistent contribution of freshwater to these specimens. Indeed, the lifecycles of our archaeological fish are not evident for at least two specimens from the Guanabara Bay (see Supplemental Material), that may have stayed close to the mangrove/freshwater shelf during the entirety of their lives rather than migrated to a marine environment. This is a major limitation of the model for reconstructing palaeotemperatures.

Regarding non-cyclical isotopic variations, although the annual range of temperature is wide, they are not constant and do not completely depend on seasonal variations. Other factors can influence this ecosystem. Upwelling activities can be at least partially responsible for the observed patterns. A minimum seasonal temperature variation of 8°C was found by Jones and Allmon (1995) for Pliocene mollusk shells in Florida over upwelling influence, similar to the minimum seasonal variation of palaeotemperature obtained from Guanabara Bay otoliths.

Our data show temperatures lower than 14°C, which might be associated with the high influence of SACW in the bay, or by the fish migration to the marine coast surroundings. Fish were captured around a mean water temperature of 19.13 (SD = 1.51), which shows that fishery was not carried out very close to the coast. However, our data points towards derived  $\delta^{18}\text{O}_{\text{oto}}$  palaeotemperature originating mostly from inside of the paleo Guanabara Bay, indicating this environment may have been colder in the Holocene. During the last transgressive period, the paleobay occupied an area of approximately 800 km<sup>2</sup>, which is twice its current size (Amador 1980). Before the 19th century landings, the numerous islands in the area acted as barriers to the currents. This gave the waters a “swampy” nature in that strip of coast to the north of the bay and could have contributed to most of the water in the bay being cooler in the past.

Holocene reconstructed water DIC reflects the general coastal conditions of this region, are within our  $\delta^{13}\text{C}_{\text{oto}}$  results and also within modern DIC oscillation of tropical coastal waters. Upwelling events are indicated by enrichments in the isotopic oxygen profiles coinciding with episodes of depletion in the isotopic carbon record.

Data obtained for Bertucci et al. (2018) using archaeological otolith of whitemouth croaker from the Angra dos Reis shellmounds overlap with our results. This is probably explained by both habitats being located around protected inlets, relatively close to the coast and

under the influence of the Santos basin's oceanographic characteristics. According to Bertucci et al (2018), the  $\delta^{18}\text{O}_{\text{oto}}$  and  $\delta^{13}\text{C}_{\text{oto}}$  data obtained from the Saquarema region under direct influence of upwelling showed seasonal variability influenced by water temperature and salinity anomalies. Such variations were explained by cold fronts and the continental and superficial drainage of fresh water. Furthermore, the high values of  $\delta^{18}\text{O}_{\text{oto}}$  and low values of  $\delta^{13}\text{C}_{\text{oto}}$  in the Saquarema Lagoon of the Holocene are a consequence of the mixing of water masses (Bertucci et al. 2018) and different palaeo-shores with a wider ranging marine environment (Amador 1980).

Our most positive  $\delta^{13}\text{C}_{\text{oto}}$  data indicates that it is possible that the Saquarema Lagoon was more saline in the Holocene in agreement with coastal geomorphologic configuration presented by Turcq (1999) and with mixed waters (Bertucci et al. 2018), where fish were caught in relatively cold waters. Although Saquarema samples presented the minimum  $\delta^{13}\text{C}_{\text{oto}}$  values, they also registered the highest values of this isotope, showing largest DIC water.

Historic data of the Saquarema Lagoon before the artificial intervention, shows uniform water masses with low salinity levels throughout the entire lagoon only when rivers flooded, for short periods of the year (Carmouze et al. 1991). The presence of intermittent upwelling was mentioned by Martin et al. (1996) and gave rise to a semi-arid microclimate in Cabo Frio. Holocene derived  $\delta^{18}\text{O}_{\text{oto}}$ -palaeotemperature reconstruction from archaeological whitemouth croaker otoliths of the Brazilian coast (Bertucci et al. 2018; this paper) point to intense temperature anomalies in the shellmounds of the Saquarema complex, consistent with coastal upwelling areas and the wide range of temperatures found for this area.

## CONCLUSION

Crystallographic analyses of aragonite in the otolith samples provides no evidence of otolith diagenesis that could have significantly altered stable and radiogenic isotope values of the Guanabara Bay specimens. Radiocarbon ages of otolith samples from the top of the Galeão shellmound corresponds to a range between 5820 and 4980 cal BP and represents the oldest chronological record of a prehistoric settlement for Guanabara Bay. The Guanabara Bay is a complex ecosystem and in spite of disagreements regarding growth marks and cyclicity of otoliths sampled, data shows large amplitudes for  $\delta^{13}\text{C}_{\text{oto}}$  and  $\delta^{18}\text{O}_{\text{oto}}$  isotopes and unclear seasonality patterns, characteristic of an upwelled zone. Data from the Saquarema Lagoon shows the best correspondence between growth zones and seasonality and indicate a strongly mixed environment in accordance with previous literature.

The whitemouth croaker of this study were probably mostly nearshore residents; however, our data indicate movements between deeper or mostly marine water masses and reinforce *Micropogonias furnieri* as excellent candidates for geochemical and palaeoceanographic studies in coastal and estuarine environments. We believe a microchemical study will be able to provide support for the possibility of wide habitats of this species.

Derived  $\delta^{18}\text{O}_{\text{oto}}$  palaeotemperatures from the Guanabara Bay and Saquarema Lagoon pointed to higher  $\delta^{18}\text{O}$  values and consequently lower temperatures in the Middle Holocene. The isotopic characterization of the coastal waters of Rio de Janeiro is necessary for a better understanding of the possible changes in isotopic patterns. Additionally, in-depth studies should bring about a more accurate understanding of the intrinsic seasonality patterns of the whitemouth croaker otoliths from Brazilian coastal regions of Rio de Janeiro. This

work can contribute to future studies aiming at the understanding of prehistoric fishing patterns of whitemouth croaker, the main fish resource of the Rio de Janeiro shellmounds. It is important to continue the research in the other shellmounds (Manitiba, Ponte do Girau and Saquarema), since these sites have different distances to the sea and the results will allow for the determination of a margin of error for correction of the uncertainty rates in shallow lagoons of the region of study.

## ACKNOWLEDGMENTS

The authors thank CAPES for funding the doctoral scholarship to Lopes MS and the AASPE laboratory from the Muséum national d'Histoire naturelle Paris by funding for isotopic analysis, the SEM captures. They also thank Sylvain Pont from the Institut de Minéralogie, de Physique des Matériaux et de Cosmochimie (IMPMC) in Paris for SEM examination. Drs. Aguinaldo Nepomuceno and Mauricio Cerda helped with general work issues. We thank Henrique Vences Barros for help with the map construction. João Paulo Felizardo helped us with doubts on statistics. The authors would like to thank the Brazilian financial agencies CNPq (Conselho Nacional de Desenvolvimento Científico e Tecnológico, 307771/2017-2, 305269/2017-8, and INCT-FNA, 464898/2014-5) and FAPERJ (Fundação Carlos Chagas Filho de Amparo à Pesquisa do Estado do Rio de Janeiro, E-26/110.138/2014 and E26/203.019/2016, 305269/2017-8) for the financial support. We also thank Daniel Lima for helping us with revisions that have improved this work. The UFF, LAC-UFF, LP&MG, Artefato, ECOPECA, MNUFRJ, and MNHN of Paris are also thanked for the access to laboratorial equipment and platforms. We appreciate the excellent comments from the reviewers and editor who contributed to the improvement of this article.

## SUPPLEMENTARY MATERIAL

To view supplementary material for this article, please visit <https://doi.org/10.1017/RDC.2022.57>

## REFERENCES

- Aguilera O, Belem AL, Angelica R, Macário K, Crapez M, Nepomuceno A, Paes E, Tenorio MC, Dias F, Souza R, Rapagna L, Carvalho C, Silva E. 2016. Fish bone diagenesis in southeastern Brazilian shell mounds and its importance for paleoenvironmental studies. *Quaternary International* 391(1):18–25.
- Albuquerque CQ, Miekeley N, Muelbert JH, Walther BD, Jaureguizar AJ. 2012. Estuarine dependency in a marine fish evaluated with otolith chemistry. *Marine Biology* 159(1):2229–2239.
- Albuquerque AL, Meyers P, Belem AL, Turcq B, Siffedine A, Mendoza U, Capilla R. 2016. Mineral and elemental indicators of post-glacial changes in sediment delivery and deposition under a western boundary upwelling system (Cabo Frio, southeastern Brazil). *Palaeogeography, Palaeoclimatology, Palaeoecology* 445(1):72–82.
- Amador ES. 1980. Unidades sedimentares Cenozóicas do Recôncavo da Baía de Guanabara. *Anais da Academia Brasileira de Ciências* 52(4):756–761.
- Barange M, Perry RI. 2009. Physical and ecological impacts of climate change relevant to marine and inland capture fisheries and aquaculture. In: Cochrane K, De Young C, Soto D, editors. *Climate change implications for fisheries and aquaculture: overview of current scientific knowledge*. Fisheries technical paper FAO 530:7–95.
- Barbosa-Guimarães M. 2011. Mudança e colapso no Litoral Fluminense: os sambaqueiros e os outros no Complexo Lagunar de Saquarema, RJ. *Revista do Museu de Arqueologia e Etnologia* 21(1):71–91.
- Béarez P, Carlier G, Lorand JP, Parodi GC. 2005. Destructive and non-destructive microanalysis of biocarbonates applied to anomalous otoliths of archaeological and modern sciaenids (Teleostei) from Peru and Chile. *Académie des sciences* 328(1):243–252.

- Begg GA, Weidman CR. 2001. Stable  $\delta^{13}\text{C}$  and  $\delta^{18}\text{O}$  isotopes in otoliths of haddock *Melanogrammus aeglefinus* from the northwest Atlantic Ocean. *Marine Ecology Progress Series* 216:223–233
- Behling H. 1995. A high-resolution Holocene pollen record from Lago do Pires, SE Brazil: vegetation, climate and fire history. *Journal of Paleolimnology* 14(1):253–268.
- Behling H. 2002. South and southeast Brazilian grasslands during Late Quaternary times: a synthesis. *Palaeogeography, Palaeoclimatology, Palaeoecology* 177(1):19–27.
- Belem AL, Castelao RM, Albuquerque ALS. 2013. Controls of subsurface temperature variability in a western boundary upwelling system. *Geophysical Research Letters* 40(1):1362–1366.
- Bertucci T, Aguilera O, Vasconcelos C, Nascimento G, Marques G, Macario K, Albuquerque C, Lima TA, Belém A. 2018. Late Holocene palaeotemperatures and palaeoenvironments in the Southeastern Brazilian coast inferred from otolith geochemistry. *Palaeogeography, Palaeoclimatology, Palaeoecology* 503(1):40–50.
- Bronk Ramsey C, Lee S. 2013. Recent and planned developments of the program OxCal. *Radiocarbon* 55(2–3):720–730.
- Campana SE, Neilson JD. 1985. Microstructure of fish otoliths. *Canadian Journal of Fishes and Aquatic Science* 42(1):1014–1032.
- Campana SE. 1984. Microstructural growth patterns in the otoliths of larval and juvenile starry flounder, *Platichthys stellatus*. *Canadian Journal of Zoology* 62:1507–1512.
- Carbonel C. 1998. Modelling of upwelling in the coastal area of Cabo Frio (Rio de Janeiro – Brazil). *Revista brasileira de oceanografia* 46(1):1–17.
- Carmouze JP, Knoppers B, Vasconcelos P. 1991. Metabolism of a subtropical Brazilian lagoon. *Biogeochemistry* 14(129):148–1991.
- Carneiro MH, de Castro PMG, Tutui SLS, Bastos GCC. 2005. Micropogonias Furnieri (Desmarest, 1823). Estoque Sudeste. In: Cergole MC, Ávila-Da-Silva AO, Rossiwongtschowski CLB, editors. *Análise das Principais Pescarias Comerciais da Região Sudeste-Sul do Brasil: Dinâmica populacional das Espécies em Exploração*. Série Documentos REVIZEE: Score Sul, São Paulo: Instituto Oceanográfico, Universidade de São Paulo. p 94–100.
- Carvalho C, Macário K, Lima T, Chanca I, Oliveira F, Alves EQ, Bertucci T, Aguilera O. 2018. Otolith-based chronology of Brazilian Shellmounds. *Radiocarbon* 56(2):489–499.
- Castro JWA, Suguio K, Seoane JCS, Cunha AMD, Dias FF. 2014. Sea-level fluctuations and coastal evolution in the state of Rio de Janeiro, southeastern Brazil. *Anais da Academia Brasileira de Ciências* 86(2):671–683.
- Catanzaro LF, Baptista-Neto JA, Guimaraes MSD, Silva CG. 2004. Distinctive sedimentary processes in Guanabara Bay – SE/Brazil, based on the analysis of echo-character (7.0 kHz). *Revista Brasileira de Geofísica* 22(1):69–83.
- Cervigón F. 1993. Los peces marinos de Venezuela. Caracas: Fundación Científica Los Roques.
- Chanton JP, Lewis FG. 1999. Plankton and dissolved inorganic carbon isotopic composition in a river-dominated estuary: Apalachicola Bay, Florida. *Estuaries* 22(3):575.
- CNSA. 2018. Cadastro Nacional de Sítios Arqueológicos. Available from: [http://portal.iphan.gov.br/sgpa/cnsa\\_detalhes.php?26729](http://portal.iphan.gov.br/sgpa/cnsa_detalhes.php?26729).
- Cook PK, Dufour E, Languille MA, Mocuta C, Reguer S, Bertrand L. 2016. Strontium speciation in archaeological otoliths. *Journal of Analytical Atomic Spectrometry* 31(3): 700–711.
- Cook PK, Mocuta C, Dufour E, Languille MA, Bertrand L. 2018. Full-section otolith microtexture imaged by local-probe X-ray diffraction. *Journal of Applied Crystallography* 51(4):1182–1196.
- Cook PK, Languille MA, Dufour E, Mocuta C, Tombret O, Fortuna F, Bertrand L. 2015. Biogenic and diagenetic indicators in archaeological and modern otoliths: Potential and limits of high definition synchrotron micro-XRF elemental mapping. *Chemical Geology* 414(1):1–15.
- Cordeiro LGM, Belem AL, Bouloubassi I, Rangel B, Sifeddine A, Capilla R. 2014. Reconstruction of Southwestern Atlantic sea surface temperatures during the last century: Cabo Frio continental shelf (Brazil). *Palaeogeography Palaeoclimatology and Palaeoecology* 415(1):225–232.
- Costa MR, Araújo FG. 2003. Use of a tropical bay in southeastern Brazil by juvenile and subadult *Micropogonias furnieri* (Perciformes, Sciaenidae). *ICES Journal of Marine Science* 60(1):268–277.
- Costa-Moreira AL. 1989. Estados tróficos da laguna de Saquarema num ciclo anual [master's dissertation]. Universidade Federal Fluminense.
- Costa-Moreira AL, Carmouze JP. 1991. La lagune de Saquarema: Hydroclimatic, seston and éléments biogéniques au cours d'un cycle annuel. *Revue d'hydrobiologie tropicale* 24(1):13–23.
- Cotovicz LC Jr., Knoppers BA, Brandini N, Costa Santos SJ, Abril G. 2015. A strong  $\text{CO}_2$  sink enhanced by eutrophication in a tropical coastal embayment (Guanabara Bay, Rio de Janeiro, Brazil). *Biogeosciences* 12(1):6125–6146.
- Cotovicz LC Jr., Knoppers BA, Deirmendjian L, Abrila G. 2019. Sources and sinks of dissolved inorganic carbon in an urban tropical coastal bay revealed by  $\delta^{13}\text{C}$ -DIC signals. *Estuarine, Coastal and Shelf Science* 220:185–195.
- Degens ET, Deuser WG, Haedrich RL. 1969. Molecular structure and composition of fish otoliths. *Marine Biology* 2(1):104–113.
- Dias R, Estrella-Martinez J, Butler P, Nederbragt A, Hall IR, Barrulas P, Maurer AF, Cardeira AM, Cleia JM, Bicho DN. 2019. Mesolithic human

- occupation and seasonality: sclerochronology,  $\delta^{18}\text{O}$  isotope geochemistry, and diagenesis verification by Raman and LA-ICP-MS analysis of *Argyrosomus regius* (meagre) sagittae otoliths from layer 1 of Cabeço da Amoreira Mesolithic shell midden (Muge, Portugal). *Archaeological and Anthropological Sciences* 11(2):409–432.
- Druffel ERM, Bauer JE, Griffin S. 2005. Input of particulate organic and dissolved inorganic carbon from the Amazon to the Atlantic Ocean. *Geochemistry, Geophysics, Geosystems* 6(3): n/a–n/a.
- Dufour E, Cappetta H, Denis A, Dauphin Y, Mariotti A. 2000. Otolith diagenesis comparing microstructural, mineralogical and geochemical data: application to Pliocene fossils from Southeastern France. *Bulletin de la Societe Geologique de France* 171(5):521–532.
- Dufour E, Gerdeaux D, Wurster CM. 2007. Whitefish (*Coregonus lavaretus*) respiration rate governs intra-otolith variation of  $\delta^{13}\text{C}$  values in Lake Annecy. *Canadian Journal of Fisheries and Aquatic Sciences* 64(12):1736–1746.
- Dufour E, Neer WV, Vermeersch PM, Patterson WP. 2018. Hydroclimatic conditions and fishing practices at Late Paleolithic Makhadma 4 (Egypt) inferred from stable isotope analysis of otoliths. *Quaternary International* 47:190–202.
- Eichler PPB, Eichler BB, Miranda LB, Pereira ERM, Kfoury PBP, Pimenta FM, Bérnago AL, Vilela CG. 2003. Benthic Foraminiferal response to variations in temperature, salinity, dissolved oxygen and organic carbon, in the Guanabara Bay, Rio de Janeiro, Brazil. *Anuário do Instituto de Geociências* 26(1):36–51.
- Figueiredo AG Jr., Toledo MB, Cordeiro RC, Godoy JMO, Silva FT, Vasconcelos SC, Dos Santos RA. 2014. Linked variations in sediment accumulation rates and sea-level in Guanabara Bay, Brazil, over the last 6000 years. *Palaeogeography, Palaeoclimatology, Palaeoecology* 415:83–90.
- Figuti L. 1993. O homem pré-histórico, o molusco e o sambaqui: considerações sobre a subsistência dos povos sambaquianos. *Revista do Museu de Arqueologia e Etnologia* 3:67–80.
- Fish SK, Deblasis P, Gaspar MD, Fish PR. 2000. Eventos incrementais na construção de sambaquis, litoral do sul do Estado de Santa Catarina. *Revista do Museu de Arqueologia e Etnologia* 10:69–87.
- Franco TP, Albuquerque CQ, Santos RS, Saint’Pierrec TD, Araújo FG. 2018. Leave forever or return home? The case of the whitemouth croaker *Micropogonias furnieri* in coastal systems of Southeastern Brazil indicated by otolith microchemistry. *Marine Environmental Research* 144(1):28–35.
- Gaspar MD. 1991. Aspectos da organização social de um grupo de pescadores, coletores e caçadores: Região compreendida entre a Ilha Grande e o delta do Paraiba do Sul, Estado do Rio de Janeiro [doctoral dissertation]. Pós-graduação em Arqueologia da Universidade de São Paulo.
- Gaspar MD. 1999. Sambaqui: arqueologia do litoral brasileiro. Rio de Janeiro: Zahar.
- Gaspar MD. 2015. Relatório de Solicitação de Liberação de Área – Programa de resgate do patrimônio arqueológico, histórico e cultural do Rio Galeão da cidade do Rio de Janeiro. Associação Amigos do Museu Nacional. p. 14.
- Gaspar MD, De Blasis P, Fish S, Fish P. 2008. Sambaqui (shell mound) societies of coastal Brazil. *Handbook of South American Archaeology* 1:319–335.
- Gaspar MD, Klokler D, Scheel-Ybert R, Bianchini GF. 2013. Sambaqui de Amourins: mesmo sítio, perspectivas diferentes. *Arqueologia de um sambaqui 30 anos depois*. *Revista del Museo de Antropología* 6:7–20.
- Gaspar MD, Klokler D, Deblasis P. 2018. Corpos e montes: arquitetura da morte e do modo de vida dos sambaqueiros. *Revista Memoraré* 5:264–282.
- Gaspar MD, Bianchini GF, Berredo AL, Lopes MS. 2019. A ocupação sambaqueira no entorno da Baía de Guanabara. *Revista de Arqueologia* 32(2):3–14.
- Gerdeaux D, Dufour E. 2012. Inferring occurrence of growth checks in pike (*Esox lucius*) scales by using sequential isotopic analysis of otoliths. *Rapid Communications in Mass Spectrometry* 26(7):785–792.
- Giovanni: NASA. 2019. The bridge between data and science v 4.33. Available from: <https://giovanni.gsfc.nasa.gov/giovanni/>.
- Grouard S. 2010. Caribbean Archaeozoology. In: Mengoni-Goñalons G, Arroyo-Cabrales J, Polaco ÓJ, Aguilar FJ, editors. *Current advances in Latin-American Archaeozoology*. Xth ICAZ International Conference. Mexico: International Council for Archaeozoology: Universidad de Buenos Aires. p. 89–109.
- Haimovici M, Ignacio JM. 2005. *Micropogonias furnieri* (Desmarest, 1823). In: Rossi CLW, Cergole MC, Ávila-da-Silva AO, editors. *Análise das principais pescarias comerciais da região Sudeste-Sul do Brasil: Dinâmica Populacional das Espécies em Exploração*. Série Documentos Revizee-Score Sul, São Paulo. p. 101–107.
- Heaton TJ, Köhler P, Butzin M, Bard E, Reimer RW, Austin WEN, Bronk-Ramsey C, Grootes PM, Hughen KA, Kromer B, Reimer PJ, Adkins J, Burke A, Cook MS, Olsen J, Skinner LC. 2020. Marine20—the marine radiocarbon age calibration curve (0–55,000 cal BP). *Radiocarbon* 62(4):779–820.
- Høie H, Folkvord A. 2006. Estimating the timing of growth rings in Atlantic cod otoliths using stable oxygen isotopes. *Journal of Fish Biology* 68(3):826–837.
- Hughen KA, Baillie MG, Bard E, Beck JW, Bertrand CJ, Blackwell PG, Buck CE, Burr GS, Cutler KB,

- Damon PE, Edwards RL, Fairbanks RG, Friedrich M, Guilderson TP, Kromer B, McCormac G, Manning S, Bronk -Ramsey C, Reimer PA, Reimer RW, Remmele S, Southon JR, Stuiver M, Talamo S, Taylor FW, Plicht JV, Weyhenmeyer CE. 2004. Marine04 marine radiocarbon age calibration, 0–26 cal kyr BP. *Radiocarbon* 46(3):1059–1086.
- Hut G. 1987. Consultants group meeting on the stable isotope reference samples for geochemical and hydrological investigations. Report to the Director General. Vienna: International Atomic Energy Agency. p. 42.
- Jones DS, Allmon WD. 1995. Records of upwelling, seasonality and growth in stable-isotope profiles of Pliocene mollusk shells from Florida. *Lethaia* 28(1):61–74.
- Kalas FA, Carreira RS, Macko SA, Wagener ALR. 2009. Molecular and isotopic characterization of the particulate organic matter from an eutrophic coastal bay in SE Brazil. *Continental Shelf Research* 29(1):2293–2302.
- Kaschner KK, Kesner-Reyes C, Garilao J, Rius-Barile T, Rees, Froese R. 2016. AquaMaps: predicted range maps for aquatic species. Available from: [www.aquamaps.org/2016](http://www.aquamaps.org/2016).
- Kerr LA, Secor DH, Kraus RT. 2007. Stable isotope ( $\delta^{13}\text{C}$  and  $\delta^{18}\text{O}$ ) and Sr/Ca composition of otoliths as proxies for environmental salinity experienced by an estuarine fish. *Marine Ecology Progress Series* 349:245–253.
- Kjerfvee B, Ribeiro CHA, Dias GTM, Filippo AM, Quaresma VS. 1997. Oceanographic characteristics of an impacted coastal bay: Baía de Guanabara, Rio de Janeiro, Brazil. *Continental Shelf Research* 17(13):1609–1643.
- Klokler D. 2016. Animal para toda Obra: fauna ritual em sambaquis. *Habitus* 14(1):21–34.
- Kneip LM, Crancio F, Francisco BHR. 1988. O Sambaqui da Beirada (Saquarema, RJ): aspectos culturais e paleoambientais. *Revista de Arqueologia* 5(1):1–54.
- Kneip LM, Pallestrini L, Crancio F, Machado LMC. 1991. As estruturas e suas inter-relações em sítios de pescador-res-coletores pré-históricos do litoral de Saquarema. RJ. *Boletim do Instituto de Arqueologia Brasileira* 5(1):1–42.
- Kneip LM, Crancio F, Magalhães RMM, Curvelo MA, Mello EMB, Machado LC, Mello CL. 2001. O Sambaqui de Manitoba I e Outros Sambaquis de Saquarema. Documento de Trabalho, série arqueologia 5(1):1–91.
- Lima TA. 1999–2000. Em busca dos frutos do mar: os pescadores-coletores do litoral centro-sul do Brasil. *Revista da Universidade de São Paulo* 44(1):270–332.
- Lopes MS, Bertucci TCP, Rapagna L, Tubino AR, Monteiro-Neto C, Tomas ARG, Tenório MC, Lima TA, Souza R, Carrillo-Brice JD, Haimovici M, Macario K, Carvalho C, Aguilera O. 2016. The path towards endangered species: prehistoric fisheries in Southeastern Brazil. *PLoS One* 11(6):e0154476.
- Lopes MS, Grouard S, Gaspar MD, Sabadine-Santos E, Bailon S, Aguilera OA. 2022. Middle Holocene marine and land-tetrapod biodiversity recovered from Galeão shell mound, Guanabara Bay, Brazil. *Quaternary International* 610:80–96.
- Macario KD, Alves EQ, Chanca IS, Oliveira FM, Carvalho C, Souza R, Aguilera O, Tenorio MC, Rapagnã LC, Douka K, Silva E. 2016. The Usiminas shellmound on the Cabo Frio Island: marine reservoir effect in an upwelling region on the coast of Brazil. *Quaternary Geochronology* 35:36–42.
- Macario KD, Souza RCCL, Trindade DC, Decco J, Lima TA, Aguilera OA, Marques NA, Alves EQ, Oliveira FM, Chanca IS, Carvalho C, Anjos RM, Pamplona FC, Silva EP. 2014. Chronological model of a Brazilian Holocene shellmound (Sambaqui da Tarioba, Rio de Janeiro, Brazil). *Radiocarbon* 56(2):489–499.
- Martin L, Suguio K, Flexor JM, Dominguez JML. 1996. Quaternary sea-level history and variation in dynamics along the central Brazilian coast: consequences on coastal plain construction. *Anais da Academia Brasileira de Ciências* 68:303–354.
- Mendonça MLTG, Godoy JM. 2004. Datação radiocarbônica de sítios arqueológicos do tipo sambaqui pela técnica de absorção de  $\text{CO}_2$ : uma alternativa à síntese benzênica. *Química Nova* 27:323–325.
- McCormac FG, Hogg AG, Blackwell PG, Buck CE, Higham TFG, Reimer PJ. 2004. SHCal04 Southern Hemisphere calibration, 0–11.0 cal kyr BP. *Radiocarbon* 46(3):1087–1092.
- Murawski SA. 1993. Climate change and marine fish distributions: forecasting from historical analogy. *Transactions of the American Fisheries Society* 122(5):647–658.
- Nakamura I, Inada T, Takeda M, Hatanaka H. 1986. Important fishes trawled off Patagonia. Tokyo: Japan Marine Fishery Resource Research Center.
- Nye JA, Link JS, Hare JA, Overholtz WJ. 2009. Changing spatial distribution of fish stocks in relation to climate and population size on the Northeast United States continental shelf. *Marine Ecology Progress Series* 393(1):111–129.
- Panfili J, Pontual H, Troadec H, Wright PJ. 2002. Manual of fish sclerochronology. Brest: IRD Institut Recherche Développement.
- Patterson WP, Smith GR, Lohmann KC. 1993. Continental paleothermometry and seasonality using the isotopic composition of aragonitic otoliths of freshwater fishes. *Geophysical Monograph* 78:191–202.
- Patterson WP. 1998. North American continental seasonality during the last millennium: high-resolution analysis of sagittal otoliths. *Palaeogeography, Palaeoclimatology, Palaeoecology* 138(1–4):271–303.



- Pinto DC. 2009. Concha sobre concha: construindo sambaquis e a paisagem no Recôncavo da Baía de Guanabara [doctoral dissertation]. Museu Nacional da Universidade Federal do Rio de Janeiro.
- Pivel MAG, Toledo FAL, Costa KB. 2010. Foraminiferal record of changes in summer monsoon precipitation at the southeastern Brazilian margin since the Last Glacial Maximum. *Revista Brasileira de Paleontologia* 13(2):79–88.
- Price GD, Wilkinson D, Hart MB, Page KN, Grimes ST. 2009. Isotopic analysis of coexisting Late Jurassic fish otoliths and molluscs: Implications for upper-ocean water temperature estimates. *Geology* 37(3):215–218.
- Reid PC, Fischer AC, Lewis-Brown E, Meredith MP, Sparrow M, Andersson AJ, Antia A, Bates NR, Bathmann U, Beaugrand G, Brix H, et al. 2009. Impacts of the oceans on climate change. *Advances in Marine Biology* 56:1–150.
- Reimer PJ, Baillie MGL, Bard E, Bayliss A, Beck JW, Blackwell PG, Bronk Ramsey C, Buck CE, Burr GS, Edwards RL, Friedrich M, Grootes PM, Guilderson TP, Hajdas I, Heaton T, Hogg AG, Hughen KA, Kaiser KF, Kromer B, McCormac FG, Manning SW, Reimer RW, Richards DA, Southon JR, Talamo S, Turney CSM, van der Plicht J, Weyhenmeyer CE. 2009. IntCal09 and Marine09 radiocarbon age calibration curves, 0–50,000 years cal BP. *Radiocarbon* 51(4):1111–1150. doi: [10.1017/S003822200034202](https://doi.org/10.1017/S003822200034202)
- R Development Core Team. 2008. R: A language and environment for statistical computing. R Foundation for Statistical Computing, Vienna, Austria, 2012. ISBN 3-900051-07-0. Available at: <http://www.R-project.org>.
- Rodrigues C, Lavrado HP, Falcão APC, Silva SHG. 2007. Distribuição da ictiofauna capturada em arrastos de fundo na Baía de Guanabara – Rio de Janeiro, Brasil. *Arqueologia Museu Nacional* 65(2):199–210.
- Sadovy Y, Severin KP. 1994. Elemental patterns in red hind (*Epinephelus guttatus*) otoliths from Bermuda and Puerto Rico reflect growth rate, not temperature. *Canadian Journal of Fisheries and Aquatic Science* 51(1):133–141.
- Santos RS, Costa MR, Araújo FG. 2017. Age and growth of the white croaker *Micropogonias furnieri* (Perciformes: Sciaenidae) in a coastal area of Southeastern Brazilian Bight. *Neotropical Ichthyology* 15(1):e160131.
- Scartascini FL, Saez M, Volpedo AV. 2016. Otoliths as a proxy for seasonality: the case of *Micropogonias furnieri* from the northern coast of San Matias Gulf, Rio Negro, Patagonia, Argentina. *Quaternary International* 373:136–142.
- Secor DH, Dean JM, Laban EH. 1992. Otolith removal and preparation for microstructural examination. In: Stevenson DK, Campana SE, editors. *Otolith microstructure examination and analysis*. Canadian Journal of Fisheries and Aquatic Sciences 117:19–57.
- Soares-Gomes A, da Gama BAP, Baptista-Neto JA, Freire DG, Cordeiro RC, Machado W, Bernardes MC, Coutinho R, Thompson F, Pereira RC. 2016. An environmental overview of Guanabara Bay, Rio de Janeiro. *Regional Studies in Marine Science, Regional Studies in Marine Science* 8(1):319–330.
- Souto DD, Lessa DVO, Albuquerque ALS, Sifeddine A, Turcq BJ, Barbosa CF. 2011. Marine sediments from Southeastern Brazilian continental shelf: a 1,200-year record of upwelling productivity. *Palaeogeography, Palaeoclimatology, Palaeoecology* 299(1–2):49–55.
- Stuiver M, Polach HA. 1977. Discussion: reporting of <sup>14</sup>C data. *Radiocarbon* 19(3):355–363. doi: [10.1017/S003822200003672](https://doi.org/10.1017/S003822200003672).
- Stuiver M, Reimer PJ. 1993. Extended <sup>14</sup>C data base and revised CALIB 3.0 <sup>14</sup>C age calibration program. *Radiocarbon* 35(1):215–230.
- Tenório MC, Pinto DC, Afonso MC. 2008. Dinâmica de ocupação, contatos e trocas no litoral do Rio de Janeiro no período de 4000 a 2000 anos antes do presente. *Arquivos do Museu Nacional* 66(2):311–321.
- Thorrold SR, Campana SE, Jones CM, Swart PK. 1997. Factors determining δ<sup>13</sup>C and δ<sup>18</sup>O fractionation in aragonitic otoliths of marine fish. *Geochim Cosmochim. Acta* 61(1): 2909–2919.
- Turcq B, Martin L, Flexor JM, Suguio K, Pierre C, Tasayco-Ortega L. 1999. Origin and evolution of the Quaternary coastal plain between Guaratiba and Cabo Frio, State of Rio de Janeiro, Brazil. In: Knoppers BA, Bidone ED, Abrão JJ, editors. *Environmental Geochemistry of Coastal Lagoon Systems of Rio de Janeiro, Brazil*. UFF/FINEP, Niterói. p. 25–46.
- Vazzoler AEAM. 1991. Síntese de conhecimentos sobre a biologia da corvina, *Micropogonias furnieri* (Desmarest, 1823), da costa do Brasil. *Atlântica* 13(1):55–74.
- Venancio IM, Belem AL, dos Santos THR, Zucchi MR, Azevedo AEG, Capilla R, Albuquerque AL. 2014. Influence of continental shelf processes in the water mass balance and productivity from stable isotope data on the Southeastern Brazilian coast. *Journal of Marine Systems* 139(1):241–247.
- Villagran XS, Klokler D, Nishida P, Gaspar MD, Deblasis P. 2010. *Lecturas Estratigráficas: Arquitectura Funerária Y Deposición De Resíduos En El Sambaquí Jabuticabeira II*. *Latin American Antiquity* 21(2):195–216.
- Volpedo AV, Cirelli AF. 2006. Otolith chemical composition as a useful tool for sciaenid stock discrimination in the south-western Atlantic. *Scientia Marina* 70(2):325–334.

World Ocean Atlas. 2018. NOAA National Centers for Environmental Information. Dataset. Available at: <https://www.ncei.noaa.gov/archive/accession/NCEI-WOA18>.

Wurster CM, Patterson WP, Stewart DJ, Stewart TJ, Bowlby JN. 2005. Thermal histories, stress, and

metabolic rates of chinook salmon in Lake Ontario: evidence from intra-otolith  $\delta^{18}\text{O}$  and  $\delta^{13}\text{C}$  values and energetics modeling. *Canadian Journal of Fisheries and Aquatic Sciences* 62(1):700–713.

## APPENDIX I

### Isotopic Results of $\delta^{13}\text{C}$ and $\delta^{18}\text{O}$

$\delta^{13}\text{C}$					
GS745	GS762	GS1073	GS1151	BS809	BS810
-4.18	-3.46	-3.68	-3.55	-5.70	-5.50
-2.62	-2.26	-1.53	-2.13	-6.00	-5.10
-0.52	-2.27	-2.04	0.04	-5.90	-5.10
-0.76	-1.79	-1.51	0.63	-5.90	-4.60
-1.08	-1.62	-1.23	0.59	-6.00	-4.30
-1.33	-1.86	-0.35	1.05	-5.50	-3.80
-1.57	-1.26	-0.38	0.51	-5.50	-3.50
-1.77	-1.08	-0.62	0.16	-5.10	-2.80
-1.17	-0.68	-0.45	1.20	-5.10	-2.70
-1.28	-0.60	-0.59	1.48	-5.00	-2.50
-1.18	-1.36	-0.95	1.38	-6.60	-3.20
-1.09	-1.67	-1.38	0.43	-6.40	-3.70
-1.01	-1.65	-1.53	-1.38	-6.80	-3.90
-0.95	-1.92	-0.94	-1.05	-7.20	-4.30
-0.96	-2.44	-1.01	-1.00	-7.50	-4.60
-0.62	-2.25	-0.57	-1.35	-7.50	-4.50
0.60	-1.93	-0.49	-0.95	-7.40	-4.10
0.75	-2.32	-0.63	-0.81	-7.70	-3.90
1.14	-1.56	-0.66	-1.04	-7.40	-4.00
1.03	-1.21	-0.91	-0.79	-7.10	-4.50
1.25	-1.82	-0.22	-0.39	-6.60	-4.80
1.23	-1.26	0.15	0.08	-6.50	-4.00
1.41	-0.65	0.28	0.66	-6.00	-2.20
1.04	-0.74	1.30	0.37	-5.70	-2.90
1.10	-0.14	2.42	0.74	-6.10	-3.60
1.17	-0.14	1.85	1.20	-6.30	-3.20
0.86	1.58	1.55	1.03	-6.80	-1.90
0.90	-0.07	0.39	0.73	-7.00	-0.30
0.68	1.15	-0.06	0.38	-7.10	-2.40
1.12	-0.42	0.50	0.09	-7.70	-2.50
1.08	0.43	0.67		-7.70	-2.10
1.37	1.60	0.28		-7.20	-1.60
1.74	0.78	-0.39		-6.30	-2.00
1.08	0.84	-0.73		-5.60	
0.72	-0.04	-0.46		-5.50	
0.76	-0.82	0.19		-5.80	
0.84	-0.43	0.28		-6.90	
1.59	-0.87	0.22		-7.60	

(Continued)

$\delta^{13}\text{C}$					
GS745	GS762	GS1073	GS1151	BS809	BS810
1.31	-1.12	-0.55		-7.90	
0.89	-1.94	0.29		-7.50	
0.70	-3.16	0.85		-7.00	
0.39		-0.60		-7.60	
0.49		-0.94		-7.00	
0.49		-0.45		-7.10	
-0.68		-5.80			
0.14		-4.60			
-0.09		-3.30			
-0.43		-3.40			
-4.20					
-5.00					
-5.30					
-5.00					
-3.80					
-1.30					
-1.50					

$\delta^{18}\text{O}$					
GS745	GS762	GS1073	GS1151	BS809	BS810
-3.00	-2.71	-4.03	-1.39	-0.80	-2.20
-1.99	-0.80	-0.32	-1.96	-0.70	-1.80
-0.75	-0.80	-2.93	-1.86	-0.60	-1.60
-0.49	-0.59	-2.61	-1.66	-0.70	-0.90
-0.23	-0.71	-2.40	-1.43	-0.70	-0.40
-0.46	-0.78	-1.05	-1.12	-0.60	0.10
-0.79	-0.98	-1.28	-1.30	-0.70	0.30
-1.43	-0.53	-0.96	-1.03	-0.60	0.60
-1.29	-0.54	-0.84	-0.67	-0.50	0.80
-0.96	-0.67	-0.59	-0.52	-0.80	0.80
-1.37	-0.67	-0.43	-0.44	-0.90	0.50
-1.13	-0.57	-0.56	-0.33	-0.80	-0.60
-0.70	-0.15	-0.33	0.42	-0.80	-0.60
-0.18	-0.26	0.22	0.19	-1.00	-1.00
-0.35	-0.45	0.15	0.58	-1.20	-1.30
-0.41	-0.10	0.30	0.45	-1.20	-1.10
-0.19	-0.69	0.21	1.37	-1.70	-0.80
-0.33	-0.74	-0.10	0.21	-2.30	-0.70
-0.67	-0.92	-0.42	-0.38	-1.60	-0.60
-0.69	-0.66	-0.71	-0.58	-1.10	-0.90
-0.27	-0.40	-0.73	-0.66	-1.00	-1.30
-0.29	-0.24	-0.08	-0.77	-0.50	-0.30
-0.81	1.64	0.24	-1.38	-0.40	0.70

(Continued)

(Continued)

$\delta^{18}\text{O}$					
GS745	GS762	GS1073	GS1151	BS809	BS810
-0.15	0.34	0.14	-0.89	-0.10	0.50
-0.63	0.31	-0.37	0.73	-0.10	0.70
-0.88	0.05	-0.88	0.03	0.00	1.50
-0.19	1.87	-0.56	0.14	-0.10	1.90
-0.34	-0.29	-0.25	0.14	-1.10	0.90
-0.88	3.09	-0.16	-0.20	-0.50	1.20
-0.76	-0.99	-0.30	-0.19	-0.90	1.10
-0.20	-0.75	-0.81		-1.00	1.30
-0.34	-0.22	-0.28		-1.10	1.10
-0.77	-0.11	0.05		-1.00	0.40
-0.24	-0.35	-0.38		-0.90	
-0.16	1.07	-0.42		-0.50	
-0.68	-0.93	-0.08		-0.40	
-0.29	0.06	0.07		-0.70	
-0.17	-0.78	-0.49		-0.90	
-0.71	-0.96	-0.85		-1.10	
-0.10	-0.69	-0.10		-1.10	
-0.18	0.00	0.23		-1.00	
-0.67		-0.94		-0.40	
-0.75		-0.55		-0.30	
-0.58		-0.02		0.00	
-0.24		0.70			
-0.68		1.30			
-0.54		1.70			
0.07		1.70			
1.30					
0.70					
0.00					
-0.10					
0.40					
1.00					
1.00					

**APPENDIX II**

Available radiocarbon data for Guanabara Bay shellmounds complex. \*Calibrated results by Pinto (2009) using the Calib Radiocarbon Calibration Program software (Stuiver and Reimer 1993), through the calibration curves Marine04 (Hughen et al. 2004) for shells samples and SHCal04 (McCormac et al. 2004) for charcoal samples. \*\*Calibrated by Beta Analytic Radiocarbon Dating Laboratory. \*\*\*Calibrated results by Gaspar et al. (2019) using the Calib Radiocarbon Calibration Program software (Stuiver and Reimer 1993), through the calibration curves Marine09 (Reimer et al. 2009) for shells samples and SHCal 04 (McCormac et al. 2004) for charcoal samples. Conventional: gas proportional counting; AMS: accelerator mass spectrometry; BS: benzene synthesis.

Site	City location	Stratigraphic reference	Laboratory	Sample no.	Material	Dating method	Calibrated data (2 sigma)	Dating reference
Amourins**	Guapimirim	270–280 cm	Beta Analytic	259890	Charcoal	AMS	4340–4080	Pinto (2009)
Amourins*	Guapimirim	300 cm	Beta Analytic	Not published	Charcoal	Conventional	3898–3577	Gaspar (1991)
Sernambetiba*	Guapimirim	Not published	CENA/USP	Not published	Shell	SB	1895–1588	Mendonça and Godoy (2004)
Sermambetiba*	Guapimirim	Not published	CENA/USP	Not published	Shell	SB	2062–1741	Mendonça and Godoy (2004)
Sermambetiba**	Guapimirim	80–90 cm	Beta Analytic	259895	Charcoal	AMS	1830–1620	Pinto (2009)
Guapi***	Guapimirim	10–20 cm	Beta Analytic	341740	Charcoal	AMS	5575–5314	Gaspar et al. (2019)
Guapi***	Guapimirim	90–100 cm	Beta Analytic	341741	Charcoal	AMS	5584–5326	Gaspar et al. (2019)
Seu Jorge***	Guapimirim	Not published	Beta Analytic	343430	Charcoal	AMS	3717–3485	Gaspar et al. (2019)
Seu Jorge***	Guapimirim	Not published	Beta Analytic	343431	Charcoal	AMS	3692–3482	Gaspar et al. (2019)
Sampaio I**	Itaboraí	280 cm	Beta Analytic	259892	Charcoal	AMS	4237–3830	Pinto (2009)
Sampaio I**	Itaboraí	170 cm	Beta Analytic	259891	Charcoal	AMS	4145–3866	Pinto (2009)
Sampaio I**	Itaboraí	20–60 cm	Beta Analytic	259893	Charcoal	Conventional	3638–3272	Pinto (2009)
São Bento***	Duque de Caxias	Not published	Beta Analytic	292143	Charcoal	Conventional	4526–4183	Gaspar et al. (2019)
Arapuã*	Guapimirim	Not published	CENA/USP	Not published	Shell	BS	3516–3156	Mendonça and Godoy (2004)
Arapuã*	Guapimirim	Not published	CENA/USP	Not published	Shell	BS	3363–2990	Mendonça and Godoy (2004)
Arapuã*	Guapimirim	Not published	CENA/USP	Not published	Shell	BS	2697–2356	Mendonça and Godoy (2004)
Rio das Pedrinhas*	Guapimirim	Not published	CENA/USP	Not published	Shell	BS	3170–2778	Mendonça and Godoy (2004)
Imenezes*	Guapimirim	Not published	CENA/USP	Not published	Shell	BS	2437–2112	Mendonça and Godoy (2004)